1972

Phase transformations in the system ZrO_2-CaO

Damri Sukhotanang

Department:

PHASE TRANSFORMATIONS IN THE SYSTEM ZrO_2-CaO

BY

DAMRI SUKHOTANANG, 1949-

A

THESIS

Presented to the Faculty of the Graduate School of the

UNIVERSITY OF MISSOURI - ROLLA

In Partial Fulfillment of the Requirements for the

Degree of

MASTER OF SCIENCE IN CERAMIC ENGINEERING

Rolla, Missouri

1972

Approved by

Charles A. Sorrell (advisor)

L. T. Bolton

Robert E. Moore

ABSTRACT

Thermal expansion, thermal hysteresis, and the monoclinic ⇄ tetragonal phase transformation of ZrO_2 have been studied with high temperature x-ray diffractometry. The initial transformation temperature in pure ZrO_2, on heating, is about 1150°C. The transformation occurs over a 100°C temperature range and thermal hysteresis occurs on heating and cooling. The mechanism of the transformation is related to preferred vibrational modes of atoms on the A_o-C_o plane of the monoclinic structure. Because the monoclinic B_o axis is parallel with the tetragonal [110] axis, structural relationships can be seen to be a controlling factor in the transformation. Initiation of the transformation is probably related to the vibrational energy of the atoms, and formation energy of tetragonal domains; hysteresis behavior is the result of development of strain energy between semi-coherent monoclinic and tetragonal domains.

The effects of addition of CaO on the monoclinic ⇄ tetragonal transformation of ZrO_2 and some phase relationships in the system ZrO_2-CaO were studied by high temperature diffractometry, and heating and quenching techniques.

Addition of 1 mole % CaO lowered the initial transformation from 1150° to 1100°C on heating and from 1050° to 1000°C on cooling. Further addition of CaO affects the hysteresis characteristics but not initiation of the mono-

clinic-tetragonal transformation.

Increasing CaO content causes widening of the hysteresis loop. This phenomenon is explained by formation of a cubic solid solution, semi-coherent with the tetragonal phase. The thermal history of the samples also affects the width of the hysteresis loops, possibly related to difference in defect concentration.

Phase equilibria of the system ZrO_2-CaO was studied in some detail. A cubic solid solution and the compound $CaZrO_3$ are stable binary phases in this system. The stability field of the cubic solid solution is wider at higher temperatures. The phase boundary of the cubic field at 20 mole % CaO is almost vertical and exists to low temperatures.

ACKNOWLEDGEMENT

The author wishes to acknowledge the aid and advice of Dr. Charles A. Sorrell, major advisor. He is also grateful to Dr. Harlan U. Anderson for his helpful discussion and to Dr. Robert E. Moore for his interest and encouragement.

The financial support provided by the Civil Service Commission of Thailand is greatly appreciated.

TABLE OF CONTENTS

LIST OF ILLUSTRATIONS

LIST OF TABLES

I. INTRODUCTION

ZrO_2 is a refractory material, with a melting point of 2680° ± 20°C (4856°F).[32] There are three well defined polymorphs of pure ZrO_2: monoclinic (P $2_1/c$), tetragonal (P $4_2/nmc$), and cubic (F m3m). The monoclinic phase is stable below about 1100°C and transforms over a 100°C temperature range to the tetragonal phase; at approximately 2370°C the tetragonal phase is changed to the cubic phase.

The monoclinic $\rightleftarrows$ tetragonal transformation of ZrO_2 has been observed by many investigators since 1929, but the results have not been in agreement with reported values for the initiation of the transformation on heating varying between 1000°C and 1180°C, and on cooling between 1060°C and 980°C.

The tetragonal $\rightleftarrows$ cubic transformation of ZrO_2 was observed initially by Smith and Cline,[14] with the transformation temperature reported to be 2285°C ± 15°C. There have since been many investigations of the tetragonal $\rightleftarrows$ cubic phase transformation,[16-19] with reported values between 2200° and 2400°C.

Although pure ZrO_2 is refractory, it cannot be used as a high-temperature structural product because of the volume change during the monoclinic $\rightleftarrows$ tetragonal transformation having a deleterious effect on the resistance to thermal shock. This transformation can be suppressed by the addition of some oxides which form cubic solid solutions, such as CeO_2, CaO , MgO, Y_2O_3. Lime, CaO, is most

commonly used for this purpose. Phase relationships in the system ZrO_2-CaO have been studied by many investigators but the results have not been in good agreement.

There are two main purposes of this study. The first is to study the monoclinic $\rightleftarrows$ tetragonal phase transformation in ZrO_2 by measuring thermal expansion of the monoclinic phase, thermal hysteresis, and the effect of CaO on the monoclinic $\rightleftarrows$ tetragonal transformation. The second is to study ZrO_2-CaO phase relationships further in order to compare subsolidus equilibria results with the literature. Experimental methods included x-ray diffraction, and high-temperature x-ray diffraction.

II. LITERATURE REVIEWS

A. The Crystal Structure of ZrO_2 Polymorphs

A1. Monoclinic ZrO_2

Stable ZrO_2 at room temperature is monoclinic, and its crystal structure has been studied by various investigators. The earliest study of the monoclinic phase was reported in 1926 by Yardley,[1] who indicated that monoclinic ZrO_2, with a density of 5.73 gm/cc, has lattice constants of a = 5.17 A°, b = 5.22 A°, c = 5.33 A°, and β = 99° 28', with axial ratios of 0.9905:1:1.0220. It was suggested that the structure is a distorted fluorite type. On the basis of Yardley's data, Na'ray Szabo[4] proposed a structure for monoclinic ZrO_2, but it had unsatisfactory packing and unreasonable bond distances. In 1950, Duwez and Odell[5] reported the lattice parameters for monoclinic ZrO_2 as a = 5.16 A°, b = 5.25 A°, c = 5.29 A°, and β = 80° 10'. McCullough and Trueblood[6] (1959) reported lattice parameters of monoclinic ZrO_2 as a = 5.169 A°, b = 5.232 A°, c = 5.341 A° (all $\pm$ 0.008 A°), and β = 99° 15' $\pm$ 10'. The monoclinic structure according to these investigators is shown in Figure 1. The monoclinic structure can be described as a distortion of the fluorite structure. The O_{II} atoms lie in a plane parallel with (100) and form a slightly distorted square array. The Zr atoms are in seven-fold coordination between the plane of O_{II} atoms and the plane of O_I atoms.

FIGURE 1A

PROJECTION OF ZrO_2 STRUCTURES ON (010).

Above: Monoclinic Phase

Below: Tetragonal Phase

Note: The broken lines show the orientational relationships between the monoclinic and the tetragonal structures.

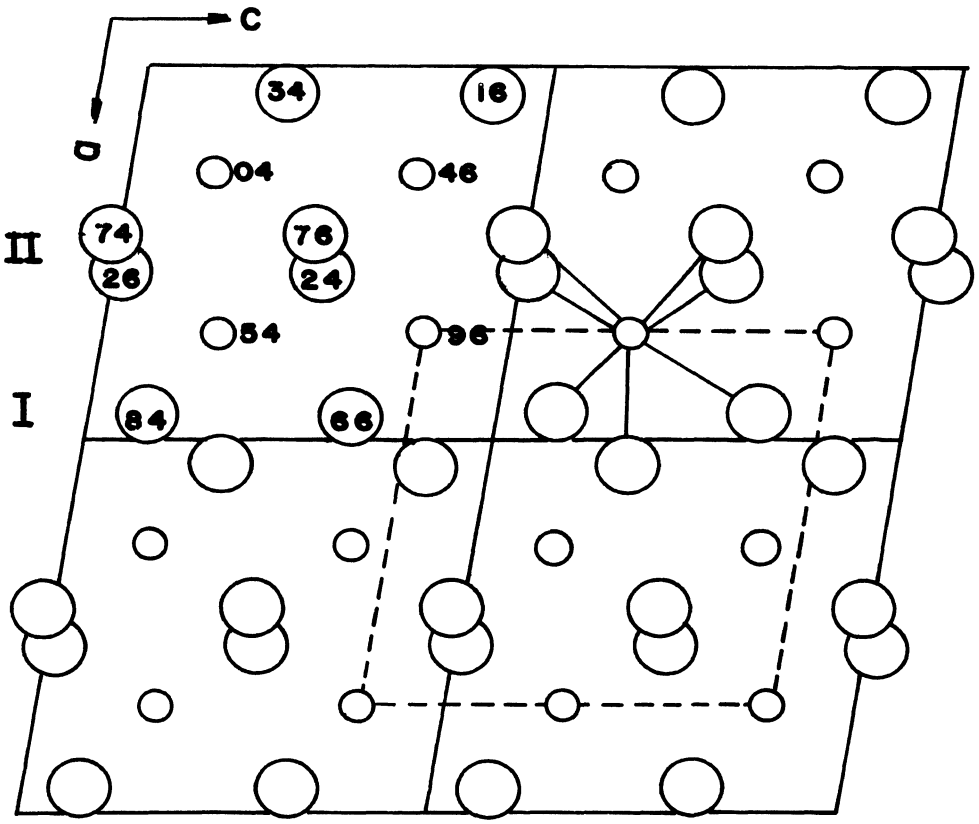

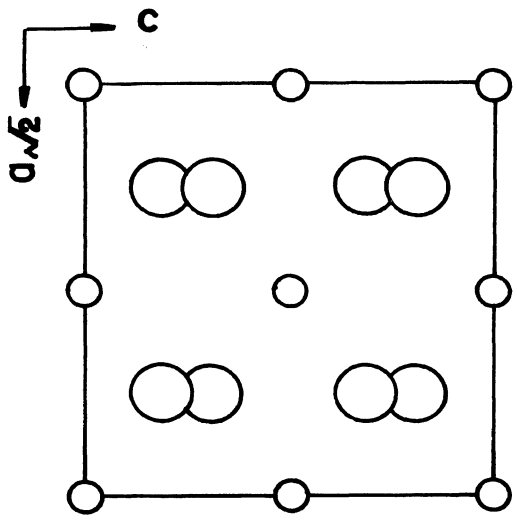

FIGURE 1a

FIGURE 1B

PROJECTION OF ZrO_2 STRUCTURES ON (001).

Above: Monoclinic Structure

Below: Tetragonal Structure

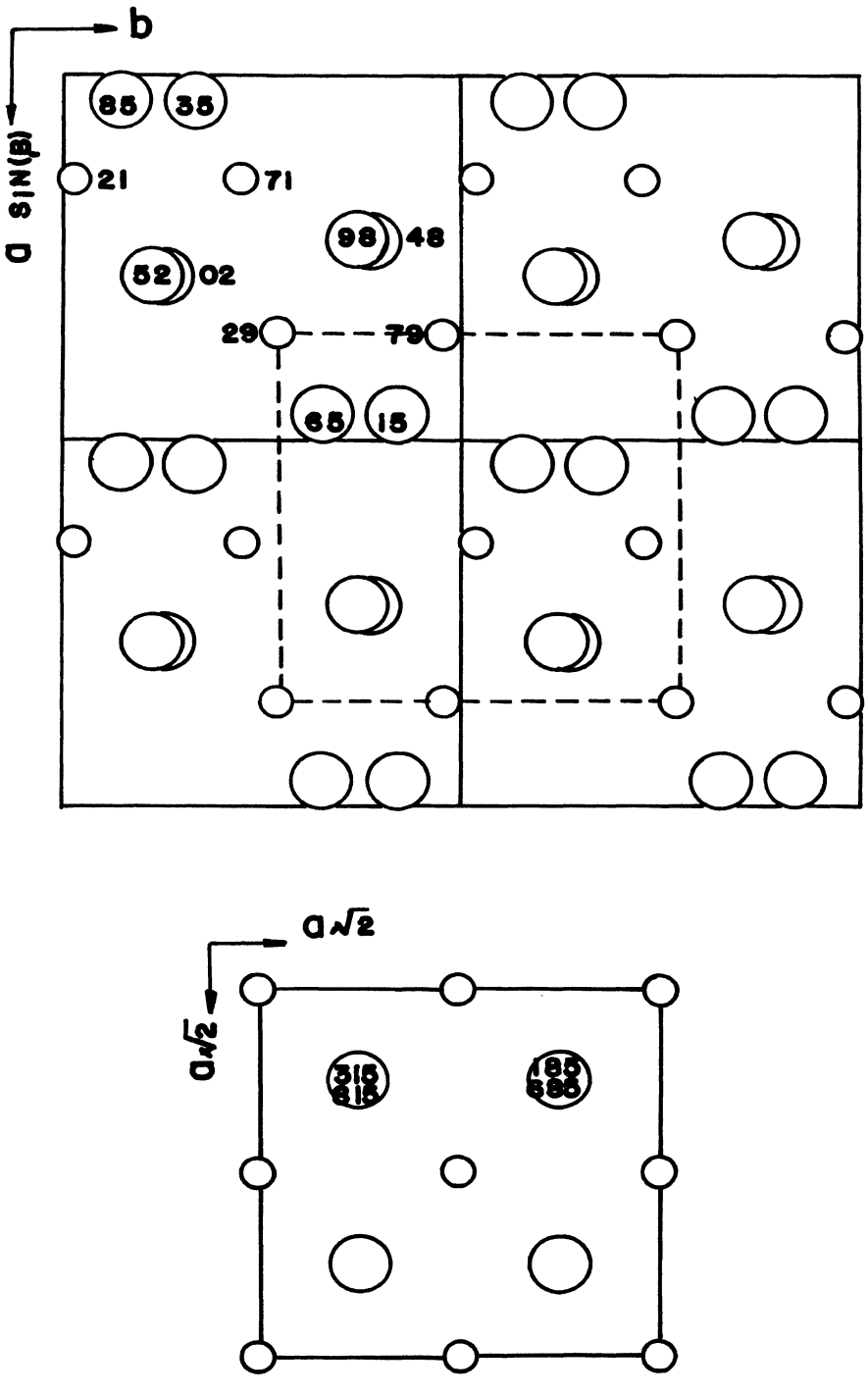

FIGURE 1b

The O_I atoms are in triangular coordination with Zr. Smith and Newkirk[7] redetermined the structure of monoclinic ZrO_2 by using new x-ray data collected from a synthetic single crystal. The results are almost the same as those of McCullough and Trueblood, with only minor changes of atomic coordinates.

A2. Tetragonal ZrO_2

The high-temperature form of ZrO_2 is tetragonal (P 4_2/nmc). The transformation occurs over a 100°C range, with wide hysteresis. In 1926 Ruff and Ebert[8] were the first investigators who reported the tetragonal form of ZrO_2, reporting that above 1000°C monoclinic ZrO_2 changed to the tetragonal form, with lattice parameters of a = 5.07 A°, c = 5.16 A°, and c/a = 1.017. For many years it was assumed that the structure of tetragonal ZrO_2 is a distorted cubic fluorite structure, as shown in Figure 1. In 1962, however, Teufer[9] redefined the structure of tetragonal ZrO_2, using a body-centered lattice instead of a face-centered tetragonal lattice as used before. The reported the lattice constants as a = 3.64 A° and c = 5.27 A° (at 1250°C), with two formular units in the elementary cell. The zirconium and oxygen atoms are located in positions similar to those in a fluorite type structure:

2 Zr (a)	0, 0, 0; 1/2, 1/2, 1/2
4 O (d)	0, 1/2, Z; 1/2, 0, $\bar{Z}$; 0, 1/2, 1/2 + Z; 1/2, 0, 1/2 - Z

where Z = 0.185

Tetragonal ZrO_2 cannot be retained on quenching, but can exist as a metastable form at room temperature if the zirconia is prepared by calcining a zirconium salt, such as the chloride or nitrate, at low temperatures.[10-13] This phenomena has been explained as the result of stabilization by residual water or anions.[13]

A3. Cubic ZrO_2

Cubic zirconia was observed in 1962 by Smith and Cline.[14] Using a high temperature x-ray diffractometer attachment, they found that above 2285° $\pm$ 15°C a cubic form was present. The tetragonal $\rightleftarrows$ cubic phase transformation was found to be rapidly reversible with hysteresis no greater than 15°C. Cubic ZrO_2 is face-centered cubic with the fluorite structure (F m3m). Because Smith and Cline used vacuum or an inert atmospheres, Weber[15] pointed out that cubic zirconia might be obtained as an oxygen-deficient product which possibly reacted with metal vapor from the furnace. Subsequently, cubic ZrO_2 has been confirmed as a polymorph or pure ZrO_2 by several investigators.[16-19] The inversion temperature of this transformation has been corrected to 2370°C.[19]

B. Mechanism of the Monoclinic $\rightleftarrows$ Tetragonal Transformation in ZrO_2

Since the monoclinic $\rightleftarrows$ tetragonal phase transformation of ZrO_2 was first reported in 1929 by Ruff and Ebert,[2] it has been the subject of many investigations. Many methods

have been employed to study the transformation: high-temperature x-ray diffraction,[16, 20-24] thermal expansion,[3, 24-25] differential thermal analysis (DTA),[22-24, 26] differential specific gravity analysis,[30] and metallographic analysis.[24] This transformation occurs over a temperature interval rather than at a sharply defined temperature, with wide hysteresis. The results of previous investigations of the monoclinic ⇄ tetragonal transformation of ZrO_2 are not in close agreement. Reported values of the initial temperature of transformation range from 1000°C to 1180°C on heating, and from 1060°C to 980°C on cooling. The characteristics of the monoclinic ⇄ tetragonal transformation in ZrO_2 are not yet fully understood. Some investigators have studied the kinetics and the thermal hysteresis of this transformation. The resulting data can be used to interpret the mechanism of the monoclinic-tetragonal phase as either a nucleation and growth process or as a martensitic shear transformation.

Wolten[16] investigated the mechanism of the monoclinic ⇄ tetragonal transformation of ZrO_2 by using high-temperature x-ray diffraction, concluding that the mechanism is of the martensitic shear type.

Smith and Newkirk[7] considered the structural relations among the ZrO_2 polymorphs. The crystallographic relationship of the monoclinic and tetragonal structures is shown in Figure 2. The major difference between the two

FIGURE 2

RELATIONSHIPS BETWEEN THE MONOCLINIC AND TETRAGONAL STRUCTURES.

Above: A layer of ZrO_7 groups of the monoclinic structure, at x = 1/4, projected on the (100) plane.

Below: One layer of ZrO_8 groups in the tetragonal ZrO_2 structure. The plane of projection is (110).

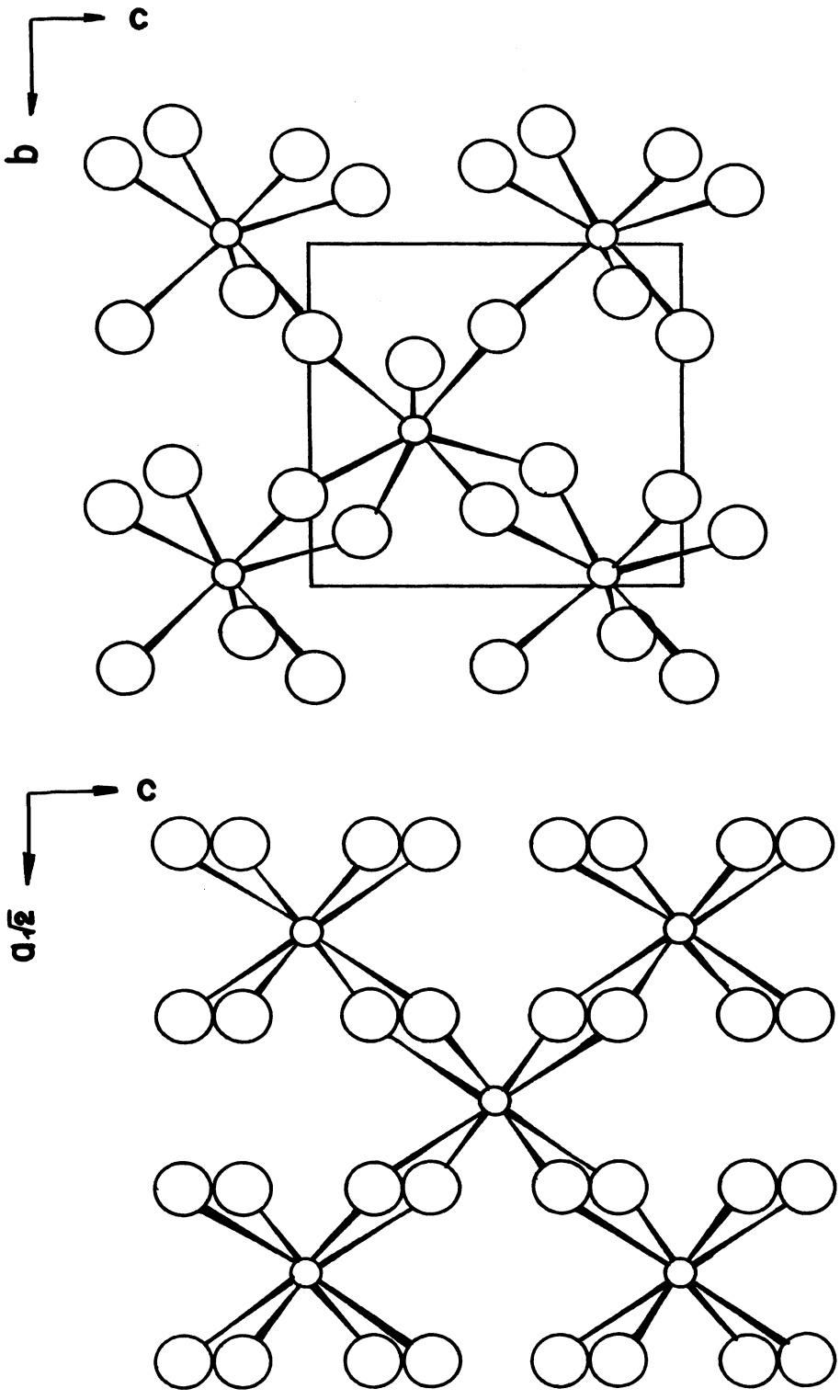

FIGURE 2

structures is the difference in the coordination of Zr-O_I atoms. Because the c axes of those two structures are parallel, they concluded that the transformation takes place by rotation of the triangular groups of O_I atoms, accompanied by minor movements of other atoms into the more symmetrical configuration.

Grain and Garvie[13] discussed the mechanism of the monoclinic $\rightleftarrows$ tetragonal phase transformation in ZrO_2 in terms of Ubbe-lohde's theory of continuous phase transformation. They commented that during the transformation, domains of the phases play the major role, with hysteresis resulting from strain energy between domains during coexistence of the monoclinic and tetragonal forms. They considered this a permissable violation of Gibbs' classical phase rule.

C. The System ZrO_2-CaO

The system ZrO_2-CaO has been studied by several investigators, the first being Ruff, Ebert, and Stephen[8] in 1929. They reported two eutectics and one compound, $CaZrO_3$, in this system. They also showed that CaO and ZrO_2 form mixed crystals with a CaO content varying from 0 to 40 mole percent. Subsequently, it was found that ZrO_2 can form cubic solid solutions with CaO.[21, 28] In 1952, Duwez, Odell and Brown,[29] restudied the system. They presented the diagram shown in Figure 3. The data were obtained from samples which had been heated to 2000°C, then annealed at various lower temperatures. Because of this,

FIGURE 3

ZrO_2-CaO PHASE DIAGRAM

From P. Duwez, F. Odell, and F.H. Brown, Jr., (1952).

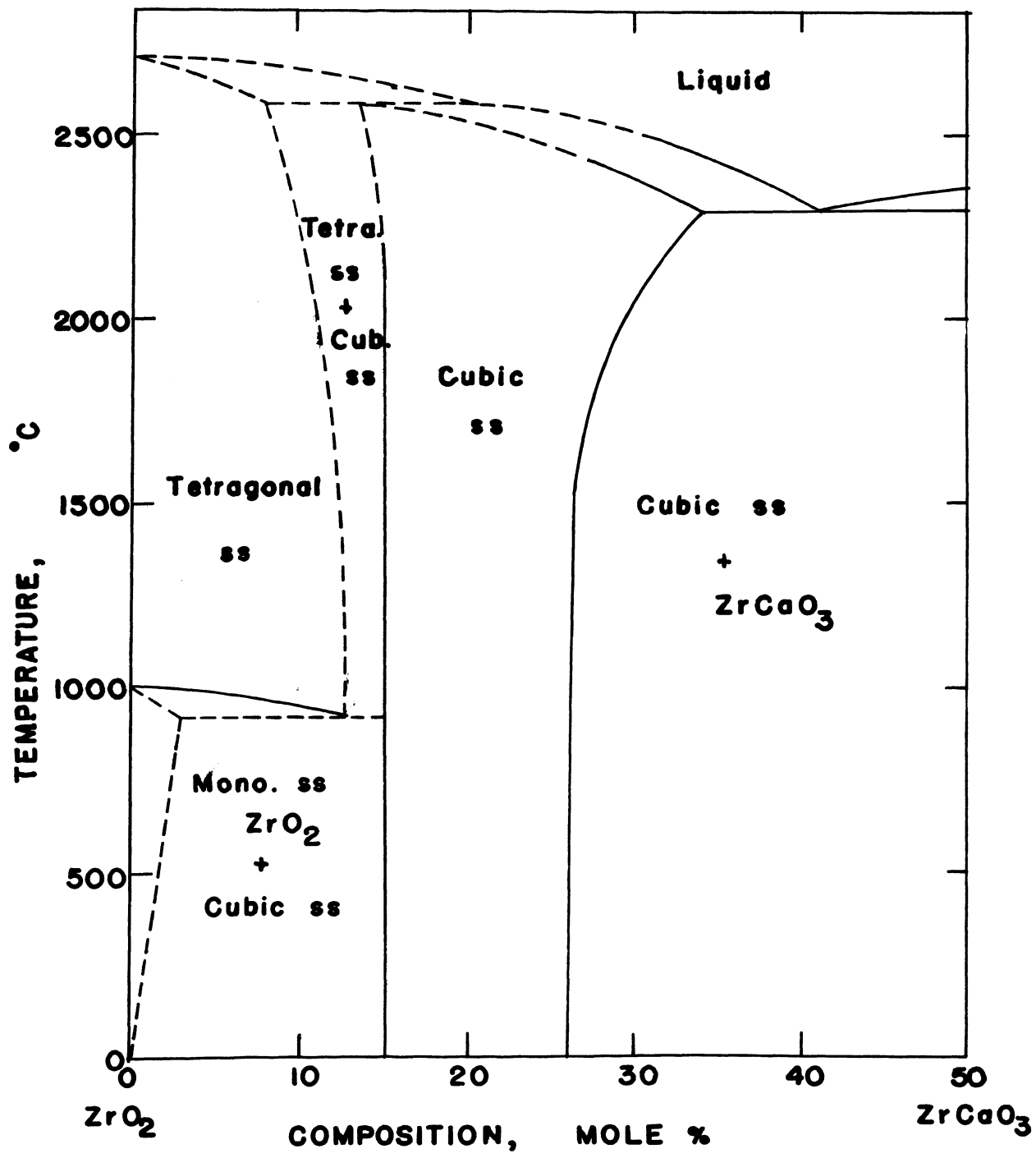
Liquid
Tetra.
ss
+
Cub.
ss
Cubic
ss
Tetragonal
ss
Cubic ss
+
ZrCaO3
Mono. ss
ZrO2
+
Cubic ss
2500
2000
1500
1000
500
0
°C
TEMPERATURE,
0
10
20
30
40
50
ZrO2
COMPOSITION, MOLE %
ZrCaO3

FIGURE 3

the results could have been in error due to the existence of metastable phases. Since that time, the system has been studied by several investigators. The results of their work can be divided into two groups. In the first group no compound was reported in the cubic field. The range of the existence of the cubic solid solution in this group is shown in Figure 4. Outside the phase boundaries are two phase regions, ZrO_2 plus cubic solid solution and the cubic solid solution plus $CaZrO_3$.

The second group of investigations reported a compound at 20 mole % CaO ($CaZr_4O_9$). The cubic fields of these investigations are shown in Figure 5. There are two phase fields outside the boundaries, ZrO_2 plus $CaZr_4O_9$ solid solutions, and $CaZr_4O_9$ plus $CaZrO_3$.

Recently work on ZrO_2-CaO phase relationships was reported by R.C. Garvie,[30] who used heating-quenching techniques. The results of his work are shown in Figure 6. He concluded from lattice parameters of cubic solid solutions that $CaZr_4O_9$ has two forms, alpha and beta, with a transformation temperature about 1650°C.

FIGURE 4

CUBIC FIELDS IN THE SYSTEM $CaO-ZrO_2$, WITH NO COMPOUND FORMATION.

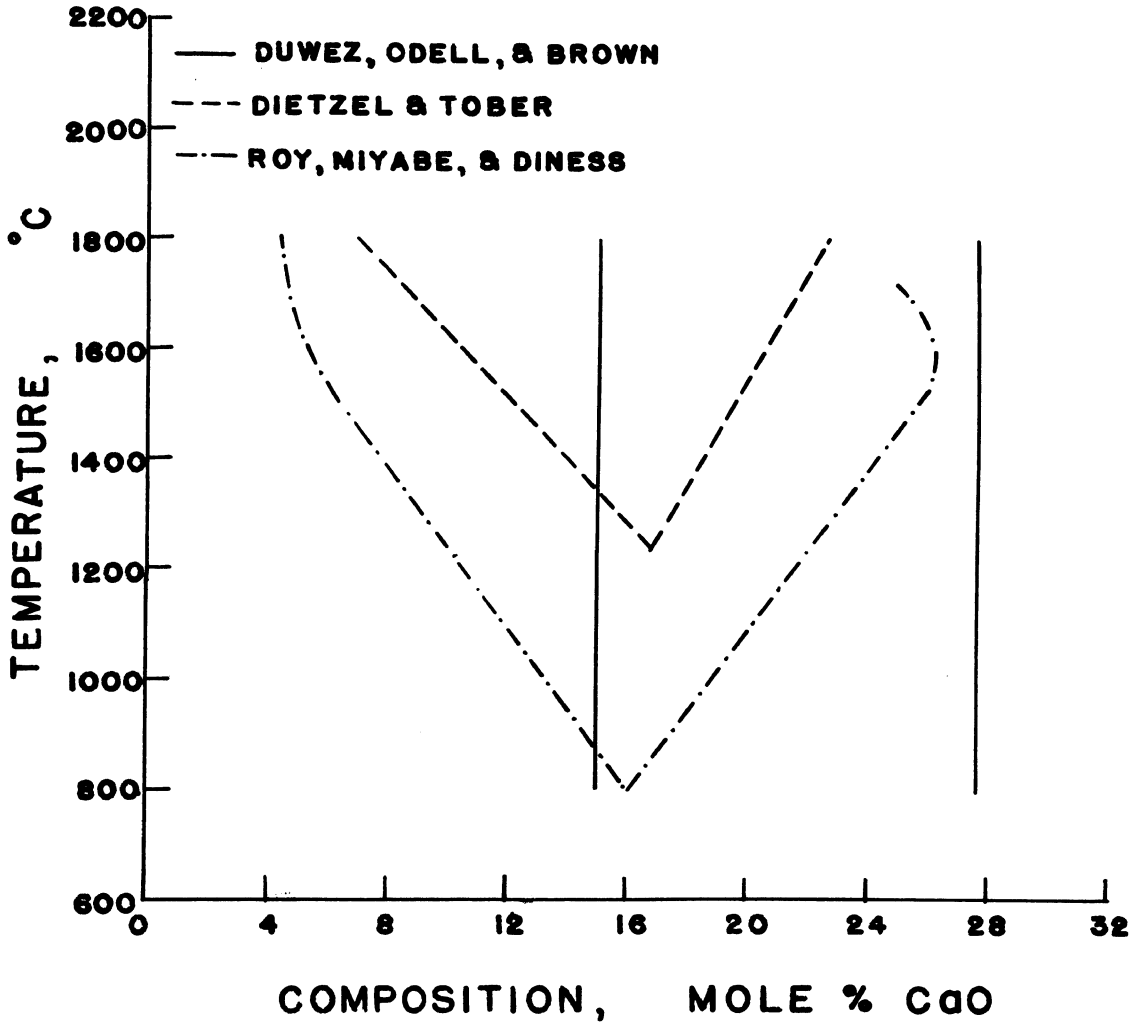
DUWEZ, ODELL, & BROWN
DIETZEL & TOBER
ROY, MIYABE, & DINESS
TEMPERATURE, °C
2200
2000
1800
1600
1400
1200
1000
800
600
0
4
8
12
16
20
24
28
32
COMPOSITION, MOLE % CaO

FIGURE 4

FIGURE 5

CUBIC FIELDS IN THE SYSTEM $CaO-ZrO_2$, WITH COMPOUND FORMATION.

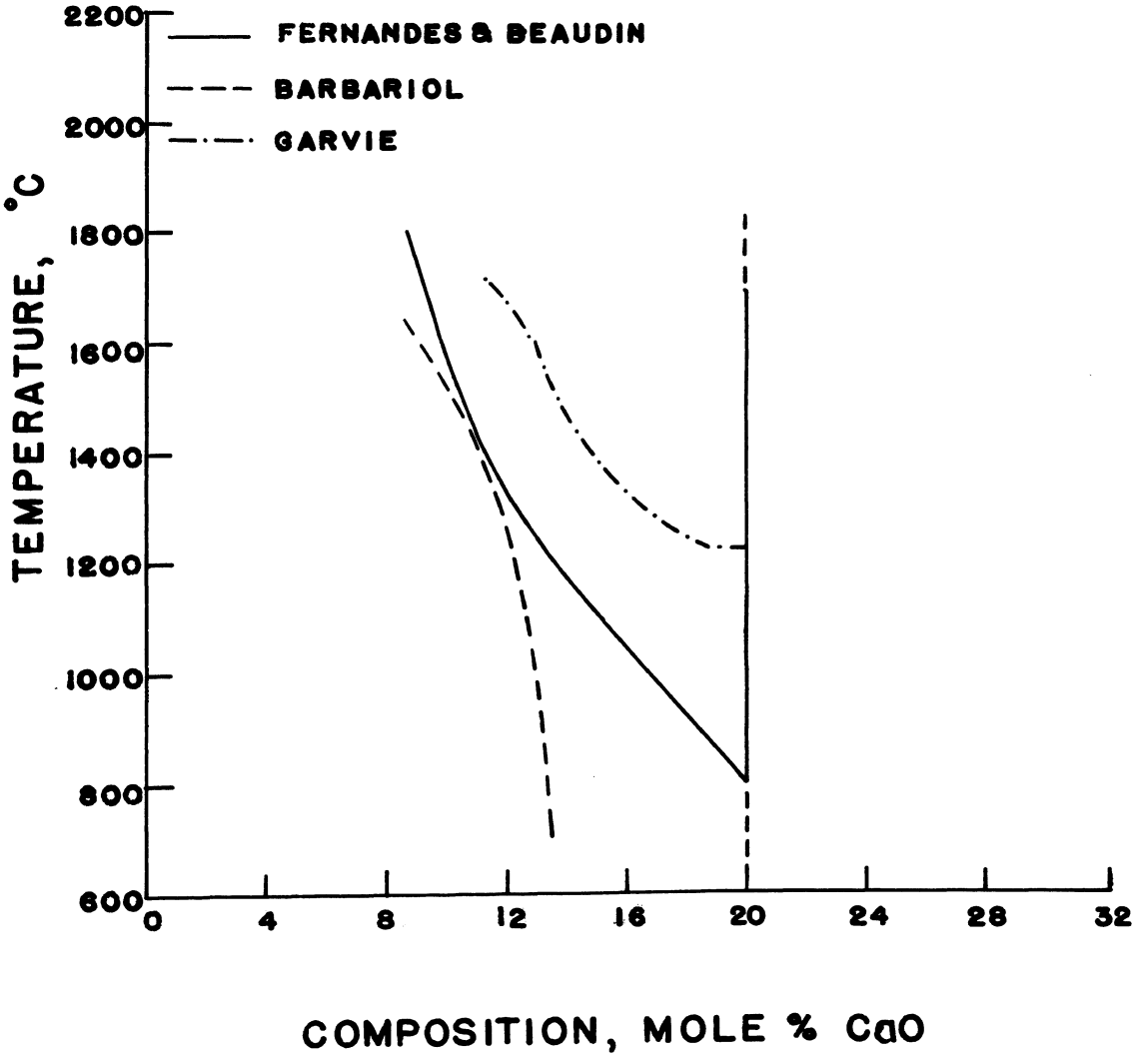
FERNANDES & BEAUDIN
BARBARIOL
GARVIE
TEMPERATURE, °C
2200
2000
1800
1600
1400
1200
1000
800
600
0
4
8
12
16
20
24
28
32
COMPOSITION, MOLE % CaO

FIGURE 5

FIGURE 6

PARTIAL PHASE DIAGRAM OF THE SYSTEM $CaO-ZrO_2$.

From R. C. Garvie (1968).

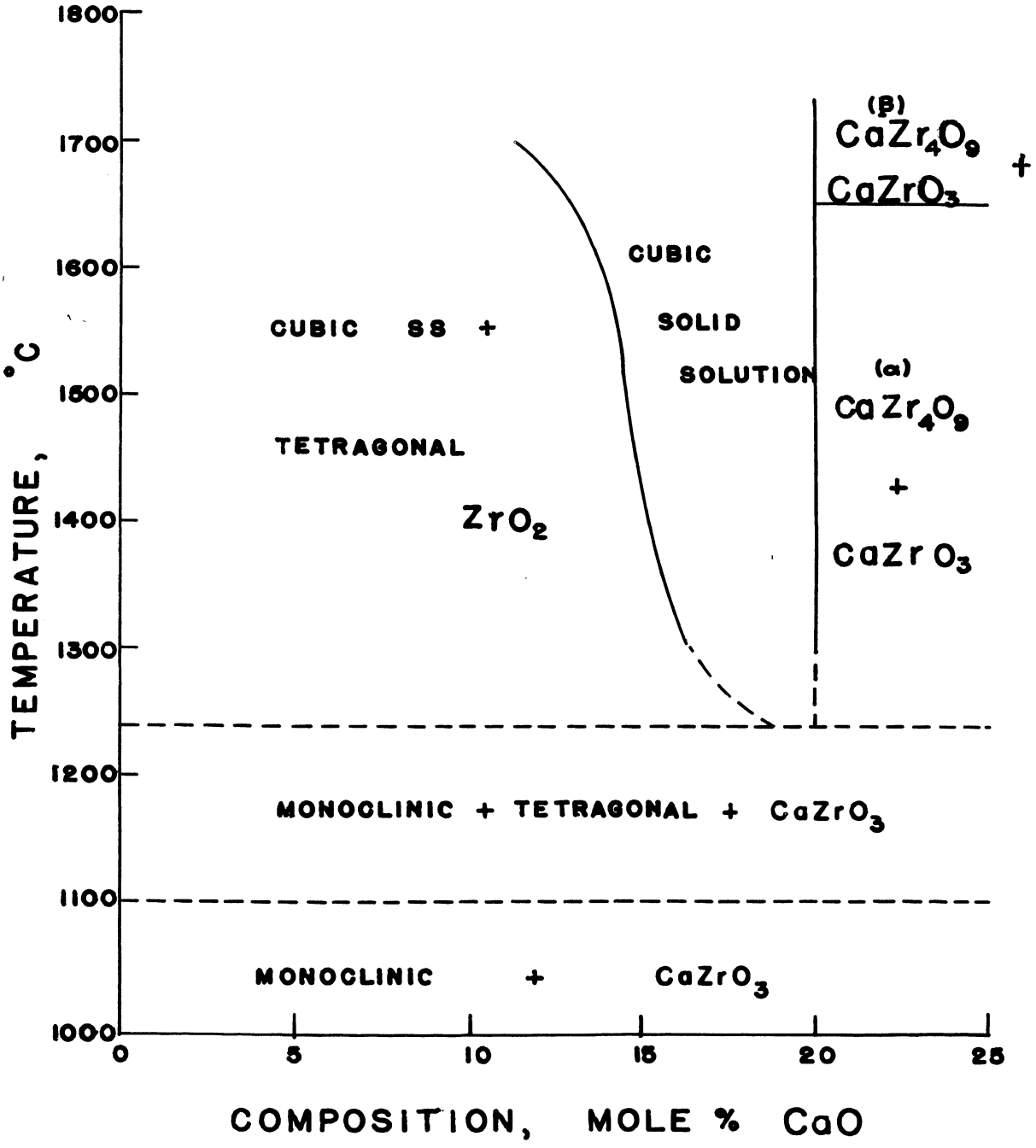
1800
1700
1600
1500
1400
1300
1200
1100
1000
°C
TEMPERATURE,
0
5
10
15
20
25
COMPOSITION, MOLE % CaO
(β)
$CaZr_4O_9$ +
$CaZrO_3$
CUBIC
SOLID
SOLUTION
CUBIC SS +
TETRAGONAL
ZrO_2
(α)
$CaZr_4O_9$
+
$CaZrO_3$
MONOCLINIC + TETRAGONAL + $CaZrO_3$
MONOCLINIC + $CaZrO_3$

FIGURE 6

III. EXPERIMENTAL PROCEDURES

A. Specimen Preparation

Pure grade zirconia powder obtained from Fisher Scientific Company was used in this investigation. Calcium carbonate powder was obtained from J.T. Baker Chemical Co. Table I shows the analysis of $CaCO_3$.

Fifty-gram samples of compositions ranging from 0.0 to 50.0 mole percent of CaO were prepared and mixed in a ball mill for 25 minutes. The compositions of the samples are shown in Table II.

Approximately 1 gm. of each sample was placed into a platinum crucible and heated in a silicon carbide resistance furnace at the desired temperature. Heating-quenching techniques were used to determine phase relationships. The samples were fired until the x-ray patterns of samples did not change, after which intensities and lattice parameters of phases were measured. Samples were heated at 1010°, 1120°, 1250°, 1310°, 1400°, and 1500°C for 2500, 2542, 768, 325, 175, 100 and 40 hours. Temperatures were controlled to within $\pm$ 10°C by a set point controller. Temperatures were measured with a Pt-Pt 13 Rh thermocouple.

High temperature x-ray techniques were used to determine thermal expansion of ZrO_2 and the effect of CaO on the monoclinic $\rightleftarrows$ tetragonal phase transformation.

B. X-ray Diffraction

TABLE I

Chemical Analysis of $CaCO_3$

	Percent
Assay ($CaCO_3$)	100.3
Insoluble in HCl	0.005
Ammonium Hydroxide Precipitate	0.005
Chloride (Cl)	0.0005
Sulfate (SO_4)	0.005
Barium (Ba)	0.001
Heavy Metals (as Pb)	0.0005
Iron (Fe)	0.0005
Magnesium (Mg)	0.005
Potassium (K)	0.009
Sodium (Na)	0.004
Strontium (Sr)	0.01

TABLE II

ZrO_2-CaO Compositions

Sample No.	Composition of CaO in mole %	in weight %
1	0.0	0.00
2	1.0	0.81
3	2.0	1.63
4	3.0	2.45
5	5.0	4.10
6	7.0	5.76
7	10.0	8.28
8	12.0	9.97
9	14.0	11.68
10	15.0	12.54
11	16.0	13.40
12	18.0	15.13
112	20.0	16.88
13	22.0	18.64
14	26.0	22.20
15	28.0	24.01
16	30.0	25.82
17	35.0	30.43
18	40.0	35.13
19	45.0	39.93
20	50.0	44.82

A G.E. XRD-5 recording diffractometer using CuKα radiation at 50KV and 15ma was used to study phase relationships. During heating and quenching cycles, samples were scanned at the rate of 2° 2θ per minute with a recording chart speed of 0.4 inch per minute. To determine intensities and the lattice parameters of the phases, samples were scanned at the rate of 0.2° 2θ per minute, using α-Al_2O_3 as an internal standard. The 2θ values of the (012), (024), and (116) lines of the Al_2O_3 and the (111), (220), and (311) lines of the cubic solid solution were determined and corrected. The lattice parameters of the cubic solid solution phase were determined from these 2θ values.

Intensities of the (111),($11\bar{1}$) of the monoclinic phase, the (111) of the cubic solid solution phase and the ($\bar{2}02$), (220) or(022), and (202) of the $CaZrO_3$ phase were measured. The percentages of the monoclinic and cubic phases were calculated by using the equation:[33]

$$x_1 = \frac{Im\ (11\bar{1}) + Im\ (111)}{Im\ (11\bar{1}) + Im\ (111) + Ic\ (111)} \times 100$$

$$x_2 = 100 - x_1$$

where x_1 = percentage of monoclinic phase in the sample

x_2 = percentage of cubic solid solution

$Im(11\bar{1})$ = the intensity of the ($11\bar{1}$) of the monoclinic phase

Im(111) = the intensity of the (111) of the monoclinic phase

$Ic(111)$ = the intensity of the (111) of the cubic solid solution

In the region of the cubic solid solution plus $CaZrO_3$ phases, the percentages of these phases were calculated from the equation:

$$x_1 = \frac{I_1}{(I_1)_o} \times 100$$

where x_1 = the percentage of the phase in the sample

I_1 = the intensity of the phase in the sample

$(I_1)_o$ = the intensity of the pure phase

A high temperature x-ray diffraction furnace was constructed for use to determine thermal expansion of ZrO_2 and thermal hysteresis. The furnace was constructed by winding externally an alumina tube, 0.4 in. inside diameter, with platinum resistance wire. This unit was cemented into an alumina shell and mounted on a water-cooled plate. This plate was bolted to a base which can be adjusted during the alignment. Figure 7 is a schematic drawing of the apparatus.

Another alumina tube, with 0.4 in. outside diameter, was cut into two parts along the length of the tube. The sample holder was a recessed platinum plate, 0.5 x 0.25 x 0.05 in., cemented onto the split tube. After the sample was loaded, the sample holder was placed in the hot zone of the furnace. Two Pt-Pt 13% Rh thermocouples were attached to the heating zone of the furnace. One was placed

FIGURE 7

HIGH-TEMPERATURE X-RAY DIFFRACTION FURNACE.

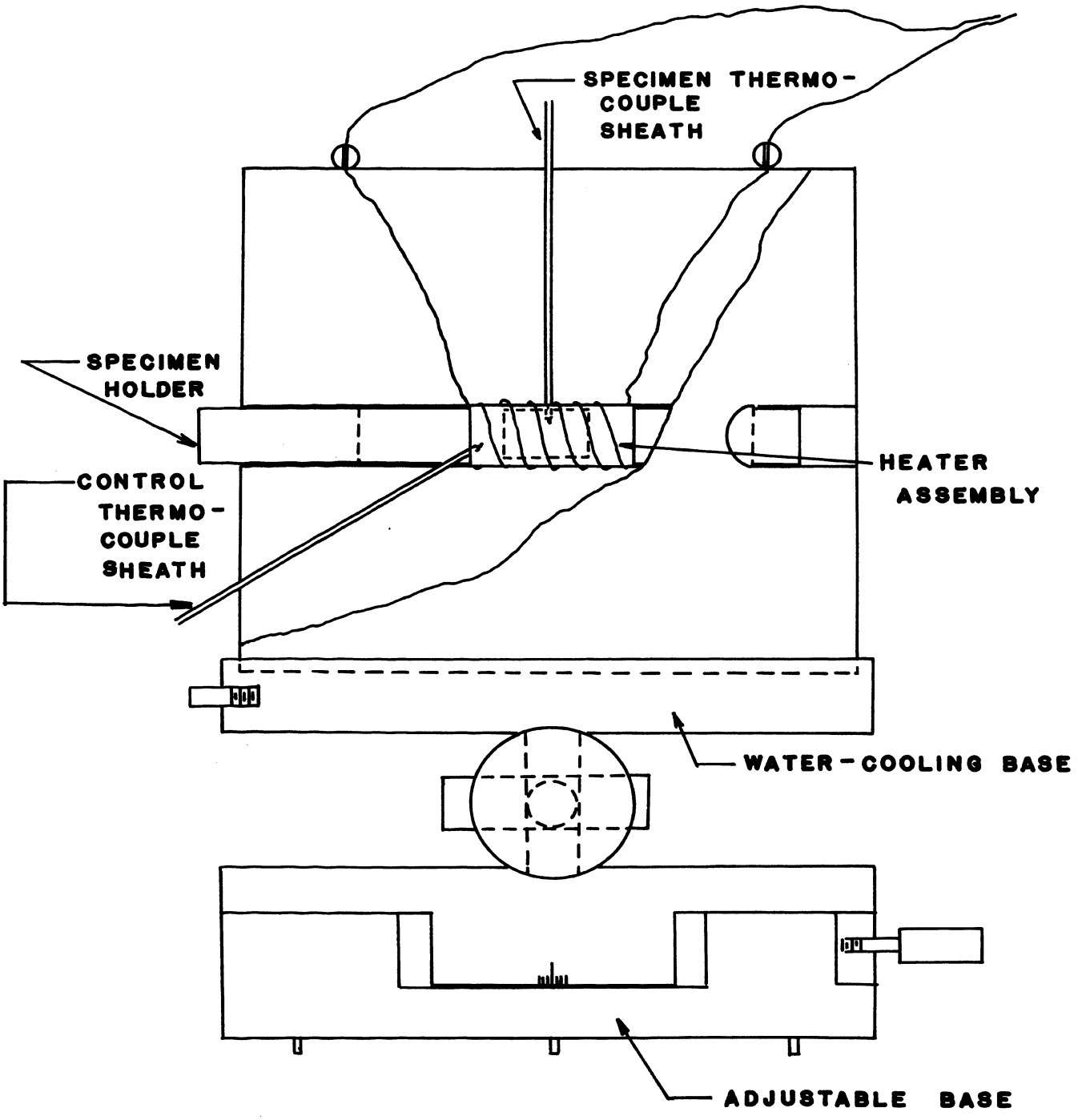
SPECIMEN THERMO-
COUPLE
SHEATH
SPECIMEN
HOLDER
CONTROL
THERMO-
COUPLE
SHEATH
HEATER
ASSEMBLY
WATER-COOLING BASE
ADJUSTABLE BASE

FIGURE 7

so that the junction was at the sample surface in the center of the hot zone, to be used to measure sample temperature with the aid of a millivolt potentiometer. The other thermocouple was used to provide emf for the temperature control system.

For thermal expansion studies the high-temperature x-ray diffraction furnace was mounted on a G.E. XRD-3 recording diffractometer. After alignment, the ZrO_2 sample was brought to temperature and maintained for about a half hour before scanning. The sample was scanned from 27° to 40° 2θ at a rate of 0.2° 2θ per minute, with a recording chart speed of 1 in. per minute. Platinum powders were mixed with the sample and the (111) line of platinum was used as an internal standard. The linear coefficient of thermal expansion of platinum is equal to 10.2×10^{-6} per degree. Thermal expansion of ZrO_2 was determined from room temperature up to 1300°C by measuring 2θ values of the (111), $(11\bar{1})$, (002), (020), and (200) lines of the monoclinic phase and the (111), (002),and (200) lines of the tetragonal phase. (Note that the indices of tetragonal phase refer to the distorted CaF_2 structure.) All measurements were made in air.

Thermal hysteresis and the effect of CaO on the monoclinic $\rightleftharpoons$ tetragonal transformation of ZrO_2 were studied by measuring the intensities of the two phases at different temperatures during transformation. The high-temperature x-ray diffraction furnace was mounted on a G.E. XRD-7 re-

cording diffractometer. Measurements of hysteresis were made in air, with temperatures ranging from 700°C to 1300°C for three heating-cooling cycles on each sample. The samples were scanned from 27° to 31° 2θ at the rate of 0.2 2θ per minute. The intensities of the (111), and $(11\bar{1})$ of the monoclinic phase and the (111) of the tetragonal phase were measured. The percentages of the tetragonal phase were calculated by using the equation:

$$x_t = \frac{I_t(111)}{Im\ (111) + I_m(11\bar{1}) + I_t(111)}$$

where x_t = percentage of the tetragonal phase

$I_t(111)$ = intensity of the (111) of the tetragonal phase

$I_m(111)$ = the same meaning as before

$I_m(11\bar{1})$ = the same meaning as before

Note: For the tetragonal phase, the (111), (002), and (200) lines, which refer to the distorted CaF_2 structure, are equal to (101), (002), and (110) lines, respectively, of the unit cell of Teufer.[9]

IV. RESULTS

A. ZrO_2 Thermal Expansion and the Monoclinic ⇄ Tetragonal Transformation

Thermal expansion of ZrO_2 was determined from 25°C to 1300°C. The five reflections, (111), (11$\bar{1}$), (002), (020), and (200), of the monoclinic phase were measured and used to evaluate the lattice parameters. The lattice parameters of the tetragonal phase were determined from the (101), (002), and (110) lines. The d-spacings and lattice parameters versus temperature are shown in Figures 8 to 12. The original data are tabulated in Appendix A. The x-ray patterns of the monoclinic and tetragonal phases are shown in Appendix B. The lattice parameters for the monoclinic phase were calculated from the equations:

$$B_o = 2\, d_{020}$$

$$A_o = 2\, d_{200}/\sin\beta$$

$$C_o = 2\, d_{002}/\sin\beta$$

$$\cos\beta = (1/d^2_{11\bar{1}} - 1/d^2_{111}) \cdot d_{002} \cdot d_{200}$$

where A_o, B_o, C_o, and β are the lattice parameters of monoclinic ZrO_2 and $d_{11\bar{1}}$, d_{111}, d_{002}, d_{020}, and d_{200} are the d-spacings of (11$\bar{1}$), (111), (002), (020), and (200) lines, respectively.

The lattice parameters of the tetragonal phase were calculated from the equations:

FIGURE 8

INTERPLANAR SPACINGS FOR (111), (11$\bar{1}$) OF MONOCLINIC ZrO_2 AND (101) OF TETRAGONAL ZrO_2 VERSUS TEMPERATURE.

Closed circles represent heating and open circles cooling.

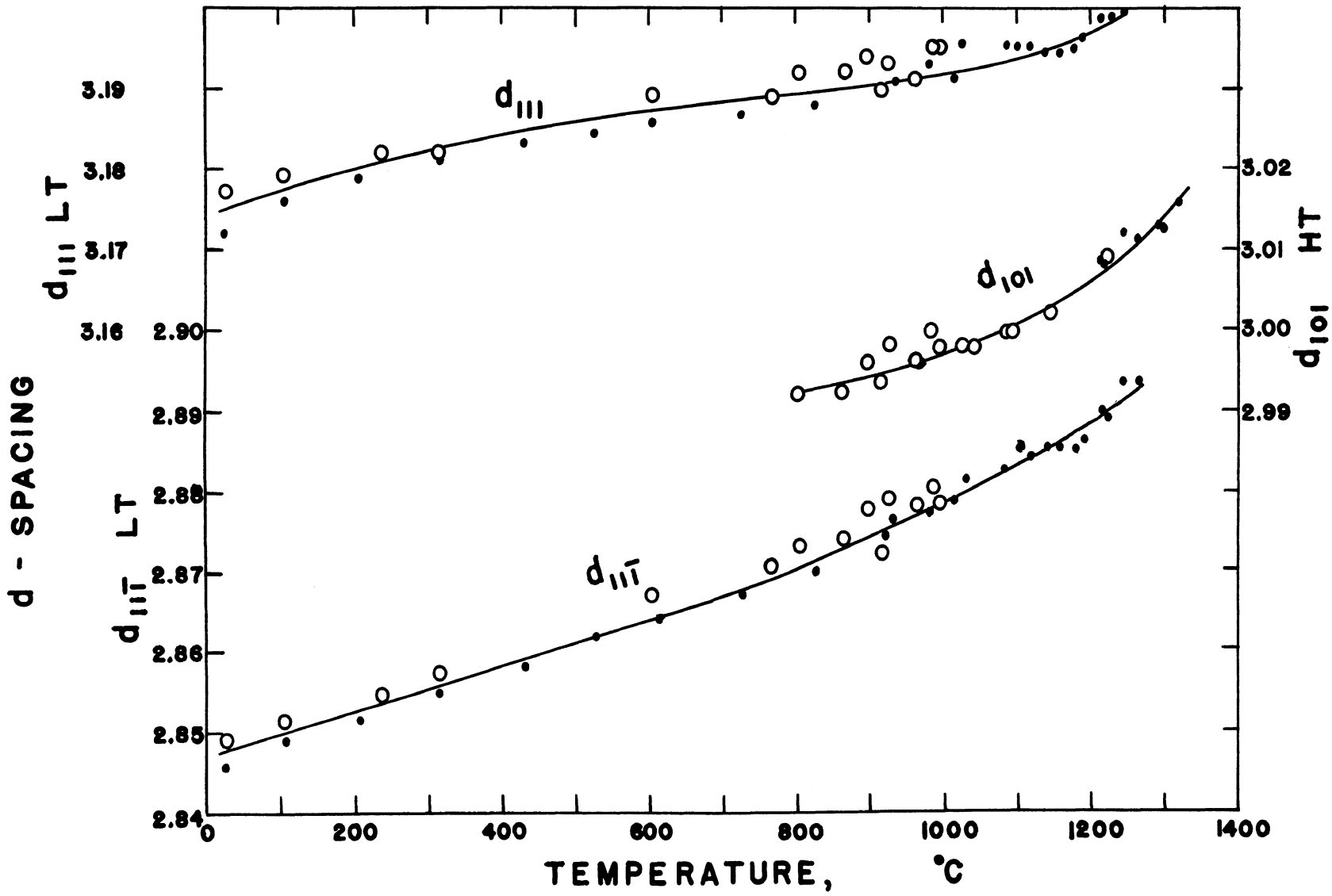
d - SPACING
d_{111} LT
$d_{11\bar{1}}$ LT
d_{101} HT
d_{111}
d_{101}
$d_{11\bar{1}}$
3.19
3.18
3.17
3.16
2.90
2.89
2.88
2.87
2.86
2.85
2.84
3.02
3.01
3.00
2.99
0
200
400
600
800
1000
1200
1400
TEMPERATURE, °C

FIGURE 8

FIGURE 9

INTERPLANAR SPACINGS FOR (020) AND (200) OF MONOCLINIC AND TETRAGONAL ZrO_2 VERSUS TEMPERATURE.

Closed circles represent heating and open circles cooling.

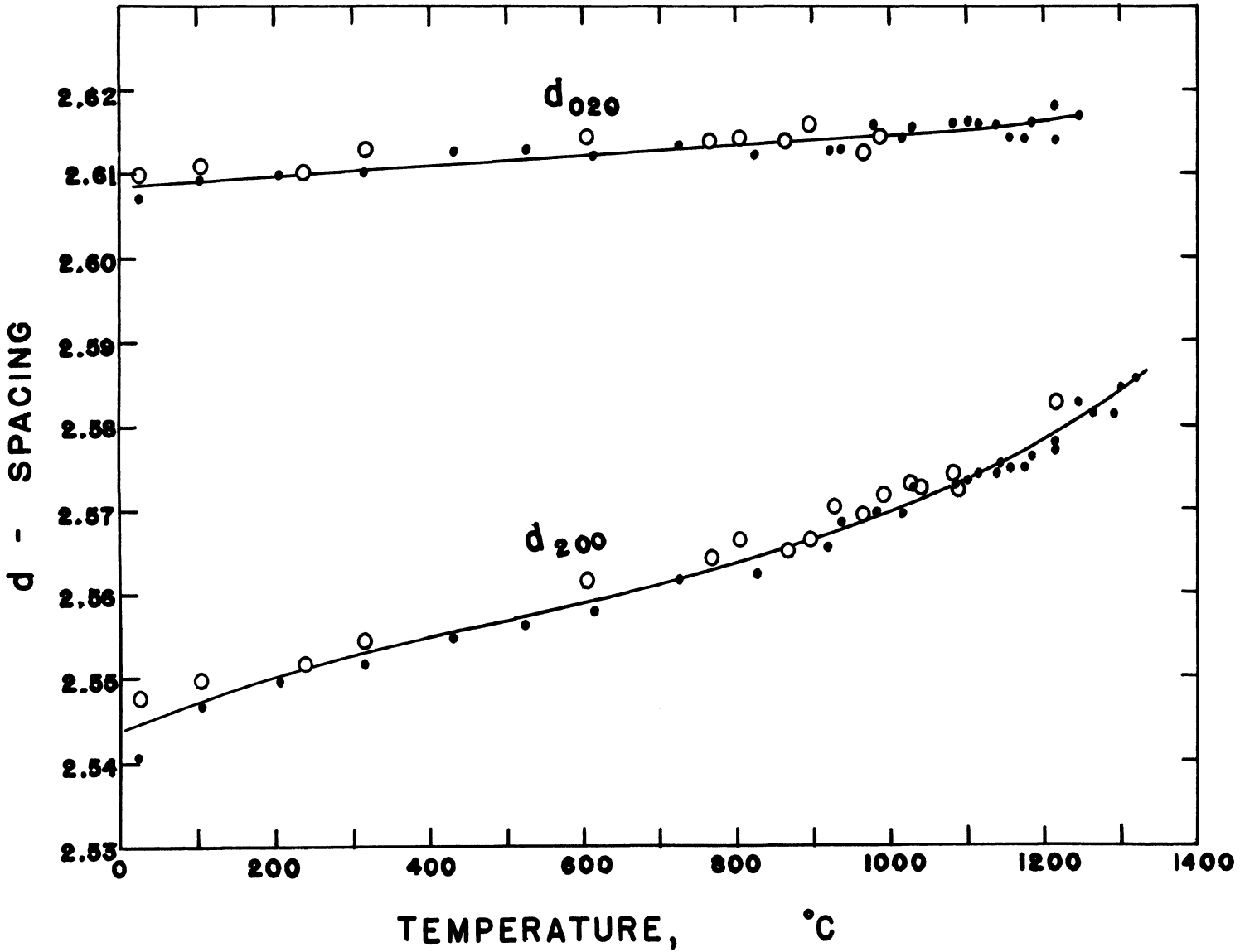
d - SPACING
2.62
2.61
2.60
2.59
2.58
2.57
2.56
2.55
2.54
2.53
0
200
400
600
800
1000
1200
1400
TEMPERATURE, °C
d_{020}
d_{200}

FIGURE 9

FIGURE 10

INTERPLANAR SPACINGS FOR (002) MONOCLINIC ZrO_2, AND (002) TETRAGONAL ZrO_2 VERSUS TEMPERATURE. Closed circles represent heating and open circles cooling.

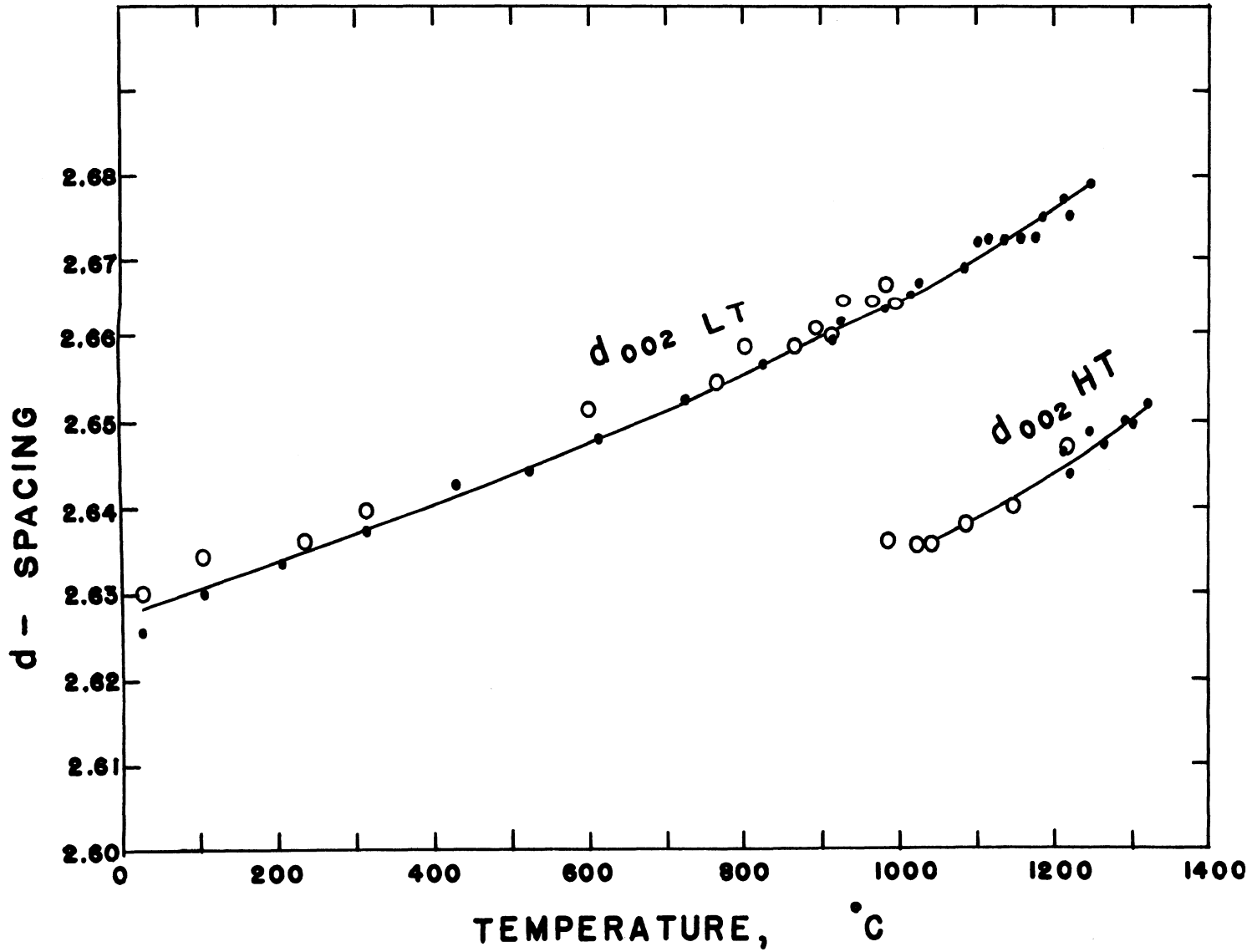
d - SPACING
2.68
2.67
2.66
2.65
2.64
2.63
2.62
2.61
2.60
0
200
400
600
800
1000
1200
1400
TEMPERATURE, °C
d 002 LT
d 002 HT

FIGURE 10

FIGURE 11

ZrO_2 LATTICE PARAMETERS IN A_o AND B_o DIRECTIONS VERSUS TEMPERATURE.

Closed circles represent heating and open circles cooling.

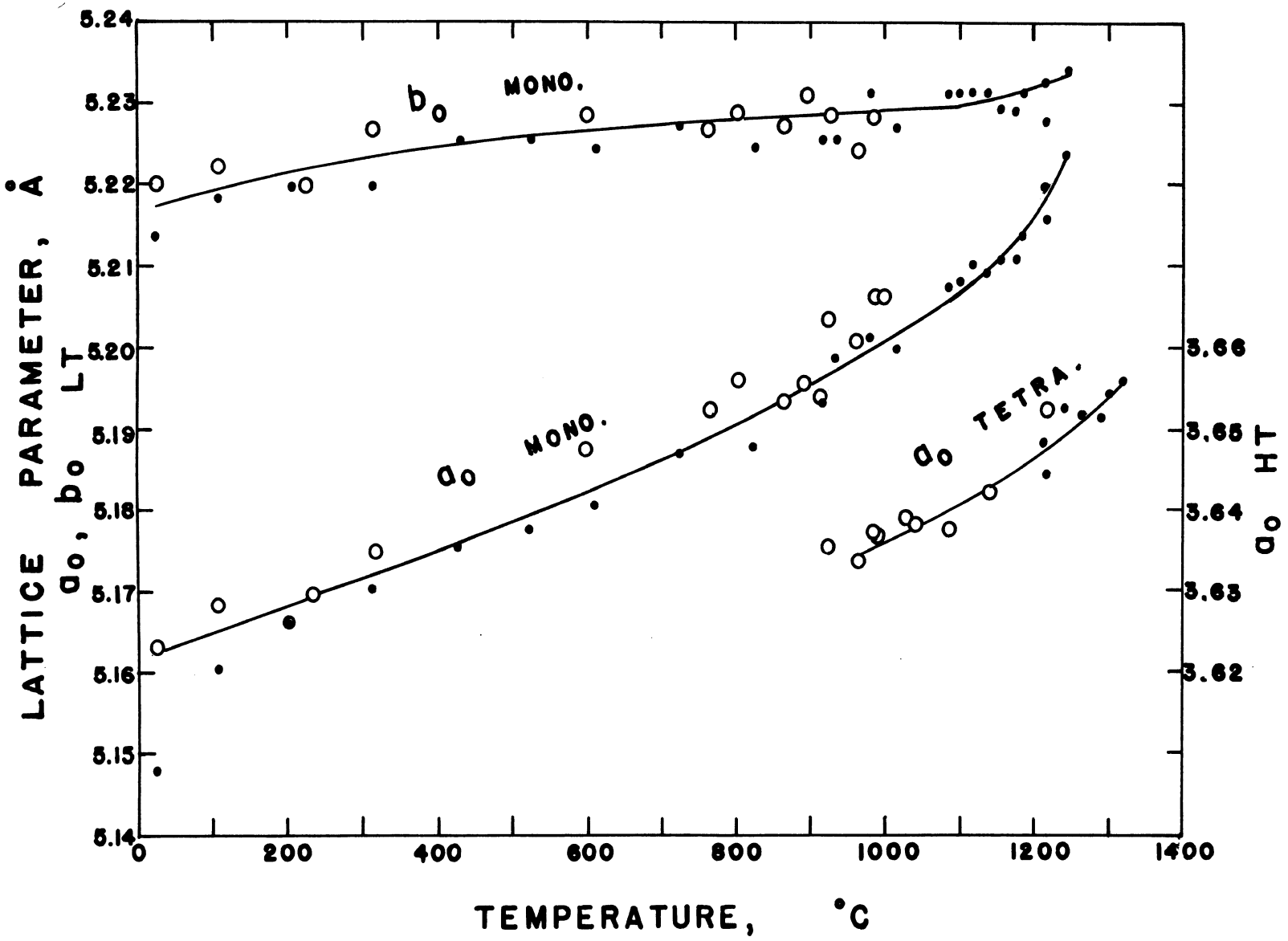
LATTICE PARAMETER, Å
a_o, b_o LT
a_o HT
TEMPERATURE, °C
b_o MONO.
a_o MONO.
a_o TETRA.
5.24
5.23
5.22
5.21
5.20
5.19
5.18
5.17
5.16
5.15
5.14
3.66
3.65
3.64
3.63
3.62
0
200
400
600
800
1000
1200
1400

FIGURE 11

FIGURE 12

ZrO_2 LATTICE PARAMETERS IN C_o DIRECTION VERSUS TEMPERATURE.

Closed circles represent heating and open circles cooling.

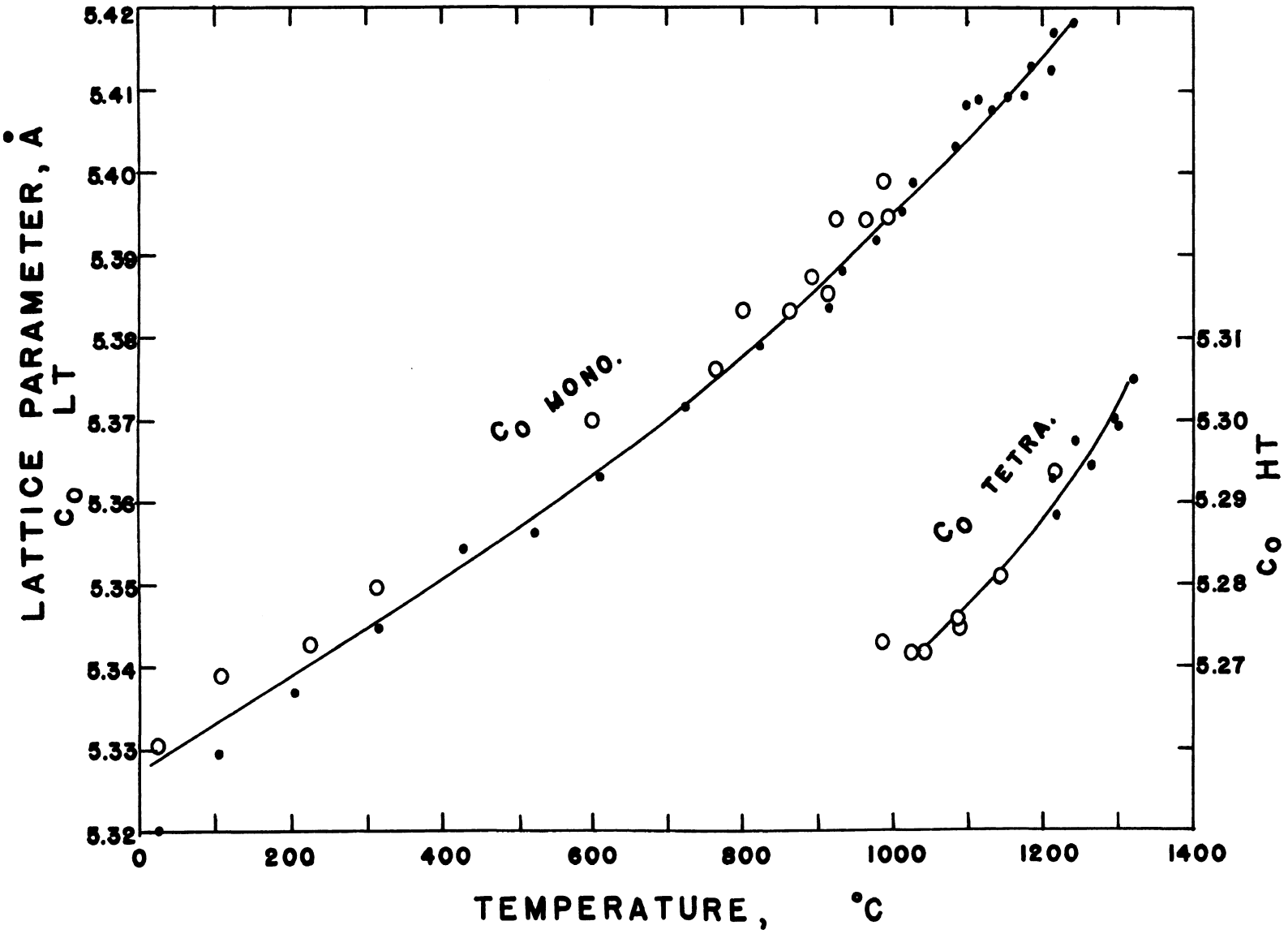
LATTICE PARAMETER, Å
Co LT
Co HT
Co MONO.
Co TETRA.
TEMPERATURE, °C
5.42
5.41
5.40
5.39
5.38
5.37
5.36
5.35
5.34
5.33
5.32
5.31
5.30
5.29
5.28
5.27
0
200
400
600
800
1000
1200
1400

FIGURE 12

$$A_o = \sqrt{2}\, d_{110}$$

$$C_o = 2\, d_{002}$$

where A_o and C_o are the lattice parameters of the tetragonal form, d_{110} and d_{002} are the d-spacings (110) and (002) lines of the tetragonal phase, respectively.

The results are in good agreement with those of Campbell and Grain,[34] but are somewhat different from those of Lang.[35] Because the sample of pure ZrO_2 used in this study had not been preheated, the values of the lattice parameter at room temperature after heating and cooling are different. The lattice parameters of the sample after one heating and cooling cycle are larger. No thermal expansion anomalies are noted; normal anisotropic expansion,with the C_o coefficient largest and the B_o coefficient smallest, is explicable on the basis of structural anisotropy. No noticeable changes in the thermal expansion curves are associated with the monoclinic-tetragonal transformation.

The transformation temperature of the monoclinic phase to the tetragonal phase was observed to be about 1150°C on heating. The low temperature form transformed over a 100°C temperature range to be the high temperature form. On cooling the monoclinic phase appeared at about 1050°C and the tetragonal phase persisted to about 600°C. During the transformation, the (002) line of the tetragonal form was observed between the (002) and the (020) lines of the monoclinic form. The (200) line of the monoclinic form

TABLE III

Linear Thermal-Expansion Coefficients

Investigator	Temp Range (°C)	(x 10^{-6})* A_o(M)	B_o(M)	C_o(M)	A_o(T)	C_o(T)
Campbell and Grain	27-264	8.4	3.0	14.0	-	-
	264-504	7.5	2.0	13.0	-	-
	504-759	6.8	1.1	11.9	-	-
	759-964	7.8	1.5	12.8	-	-
	964-1110	8.7	1.9	13.6	-	-
S.M. Lang	1150-1250	-	-	-	12.4	14.4
This Work	25-225	11.2	4.3	11.3	-	-
	225-525	6.3	2.6	11.8	-	-
	525-775	8.5	1.1	13.0	-	-
	775-975	10.7	1.3	15.3	-	-
	975-1125	9.6	2.8	17.3	-	-
	1150-1250	-	-	-	20.8	22.7

* α (T) = $\Delta l/l(T)\ \Delta T$

where: T = average temperature

ΔT = temperature interval

l = lattice constant measured

increased in intensity, due to an increase in the percentage of the tetragonal form, because of coincidence with the (110) line of the tetragonal phase. The lattice parameters of the tetragonal phase are smaller than those of the monoclinic phase within the transformation range. The transformation temperature of the monoclinic to the tetragonal form on heating is not the same as the reverse transformation on cooling. Thus heating and cooling cycles through the transformation produce a time-independent thermal hysteresis loop.

The history of the sample has some effect on the shape of hysteresis loop and on the transformation characteristics. Figure 13 shows representative hysteresis loops of the zirconia with and without previous heat treatment. Percentages of the tetragonal phase were calculated by the polymorph method, as discussed in experimental procedure. It can be seen that the hysteresis loop of the sample preheated at 1400°C for 100 hours exhibits the narrower loop and has the higher transformation temperature on cooling. On heating the transformation of these two samples started almost at the same temperature, around 1150°C, but the tail of the hysteresis loop of the non-preheated sample is longer than that of the preheated sample. On cooling the reverse transformation of the preheated sample started at about 1090°C, 40°C higher than that of the non-preheated sample. The original data for these are tabulated in Appendix C.

FIGURE 13

ZrO_2 THERMAL HYSTERESIS LOOP.

Figure represents the hysteresis loops obtained from a previously unheated sample and a sample preheated at 1400°C. Closed circles represent heating and open circles cooling.

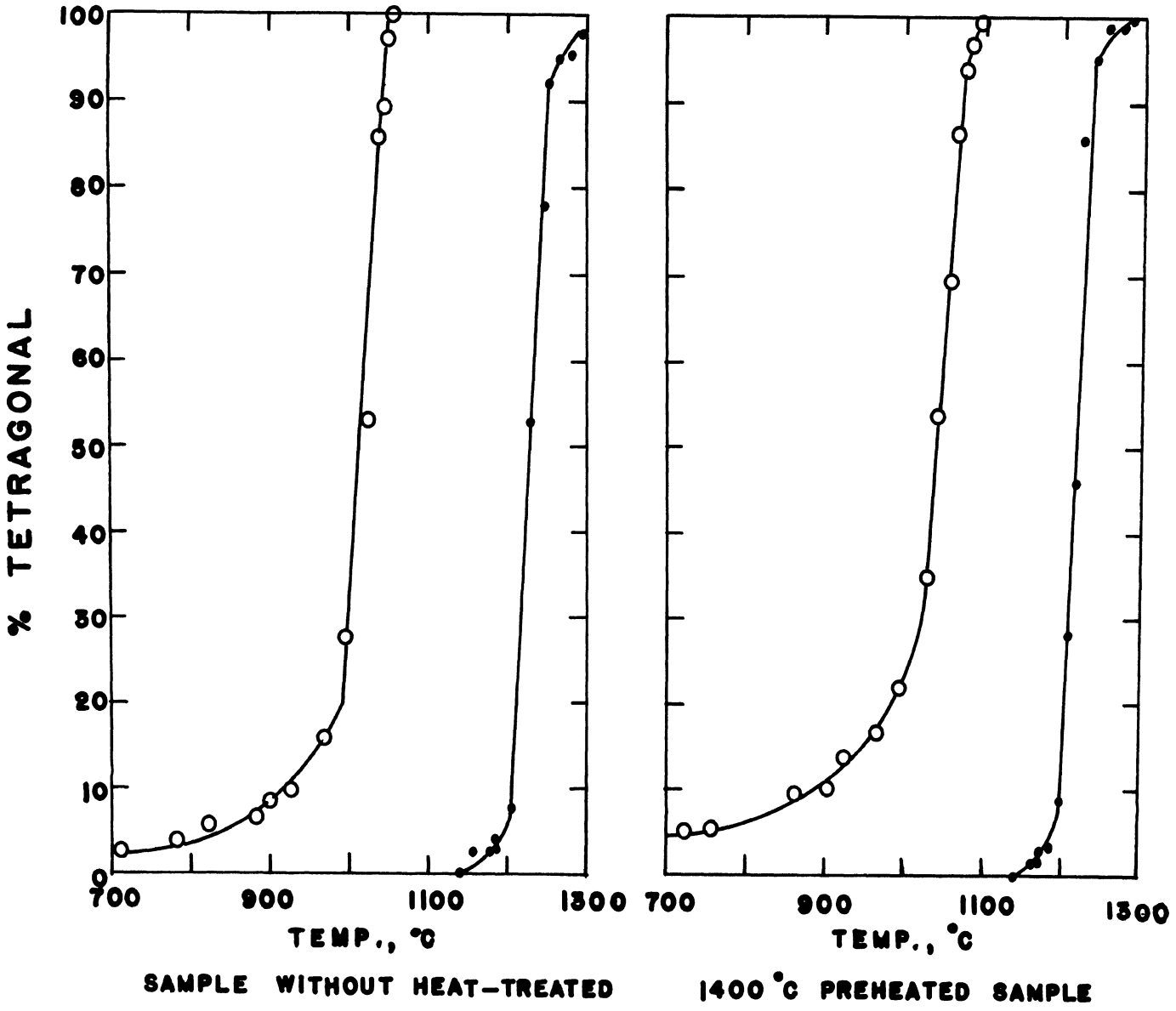
% TETRAGONAL
100
90
80
70
60
50
40
30
20
10
0
700
900
1100
1300
TEMP., °C
SAMPLE WITHOUT HEAT-TREATED
700
900
1100
1300
TEMP., °C
1400 °C PREHEATED SAMPLE

FIGURE 13

B. Effects of CaO on Thermal Hysteresis of the Monoclinic ⇄ Tetragonal Transformation

The first, in 1947, to report the effect of calcia on the inversion temperature of zirconia was Curtis.[36] In 1952, Duwez, Odell, and Brown[29] reported the effect of calcia on the transformation temperature of zirconia on cooling. The results of these two groups of investigations are in good agreement. They reported that the effect of calcia, up to about 16% mole percent, is to decrease slightly the inversion temperature. The transformation temperature of zirconia on cooling decreased from 1000° to 900°C with an increase of calcia content from 0 to 15 mole percent.

In this investigation, thermal hysteresis of ZrO_2 with additions of CaO was studied. Samples of ZrO_2 with 1, 2, 5, 7, 10, and 12 mole % CaO, preheated at 1250°C for 325 hours, were scanned through the transformation range and percentages of the tetragonal phase were measured. The resulting hysteresis loops are shown in Figures 14 to 16. The original data are also tabulated in Appendix C.

Minor amounts of CaO added to the ZrO_2 have a major effect on the transformation temperature and on transformation characteristics. Addition of 1 mole % CaO reduced the monoclinic - tetragonal transformation temperature from 1150°C to about 1100°C. Development of the tetragonal phase was complete at about 1250°C. On cooling

FIGURE 14

THERMAL HYSTERESIS LOOPS OF 1 MOLE % AND 2 MOLE % CaO SAMPLES.

The hysteresis loop is obtained by plotting the percentages of the tetragonal form versus temperature. Closed circles represent heating and open circles cooling.

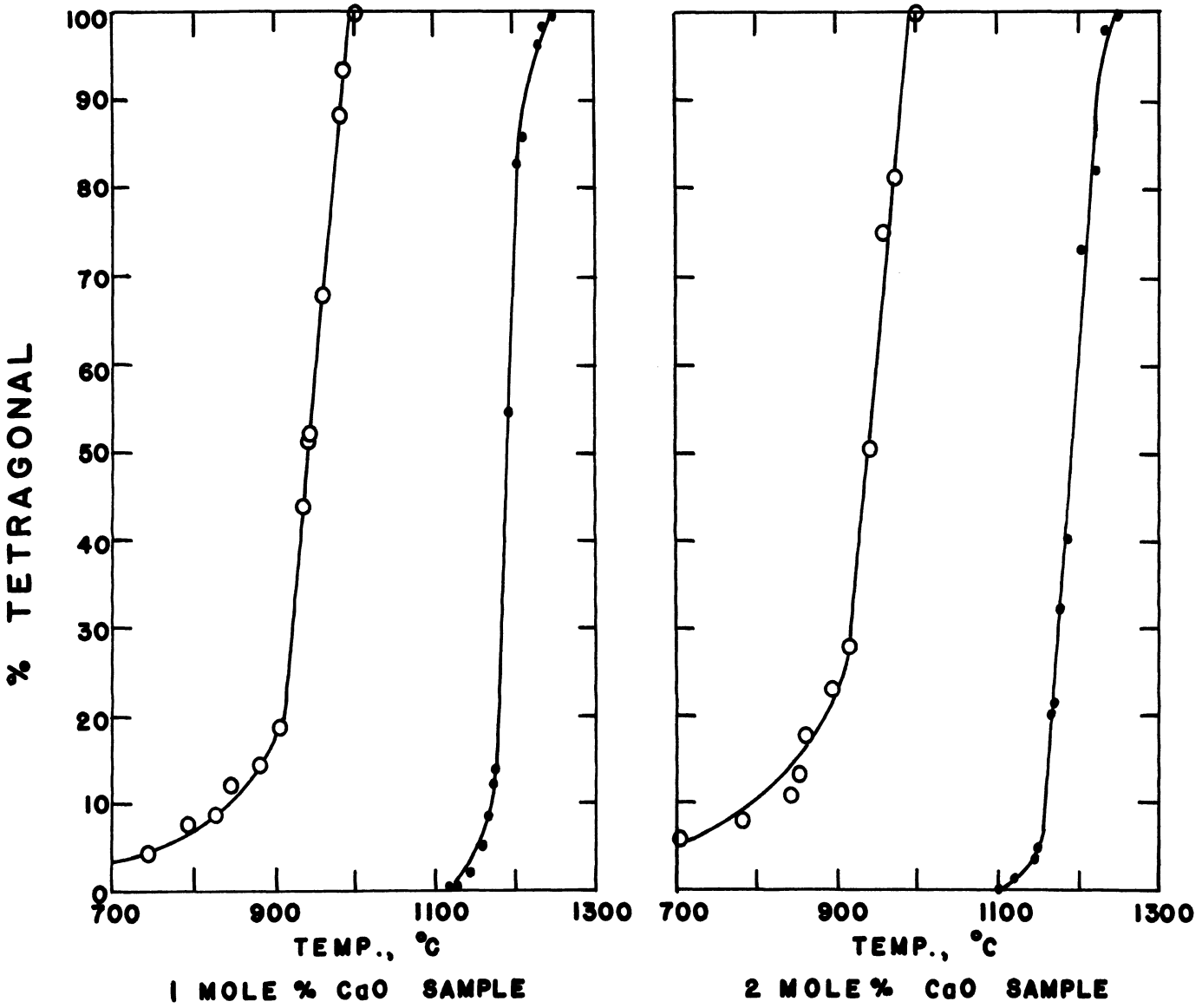
% TETRAGONAL
100
90
80
70
60
50
40
30
20
10
0
700
900
1100
1300
TEMP., °C
1 MOLE % CaO SAMPLE
700
900
1100
1300
TEMP., °C
2 MOLE % CaO SAMPLE

FIGURE 14

FIGURE 15

THERMAL HYSTERESIS LOOPS OF 5 MOLE % AND 7 MOLE % CaO SAMPLES.

Data obtained in same manner as for Figure 14.

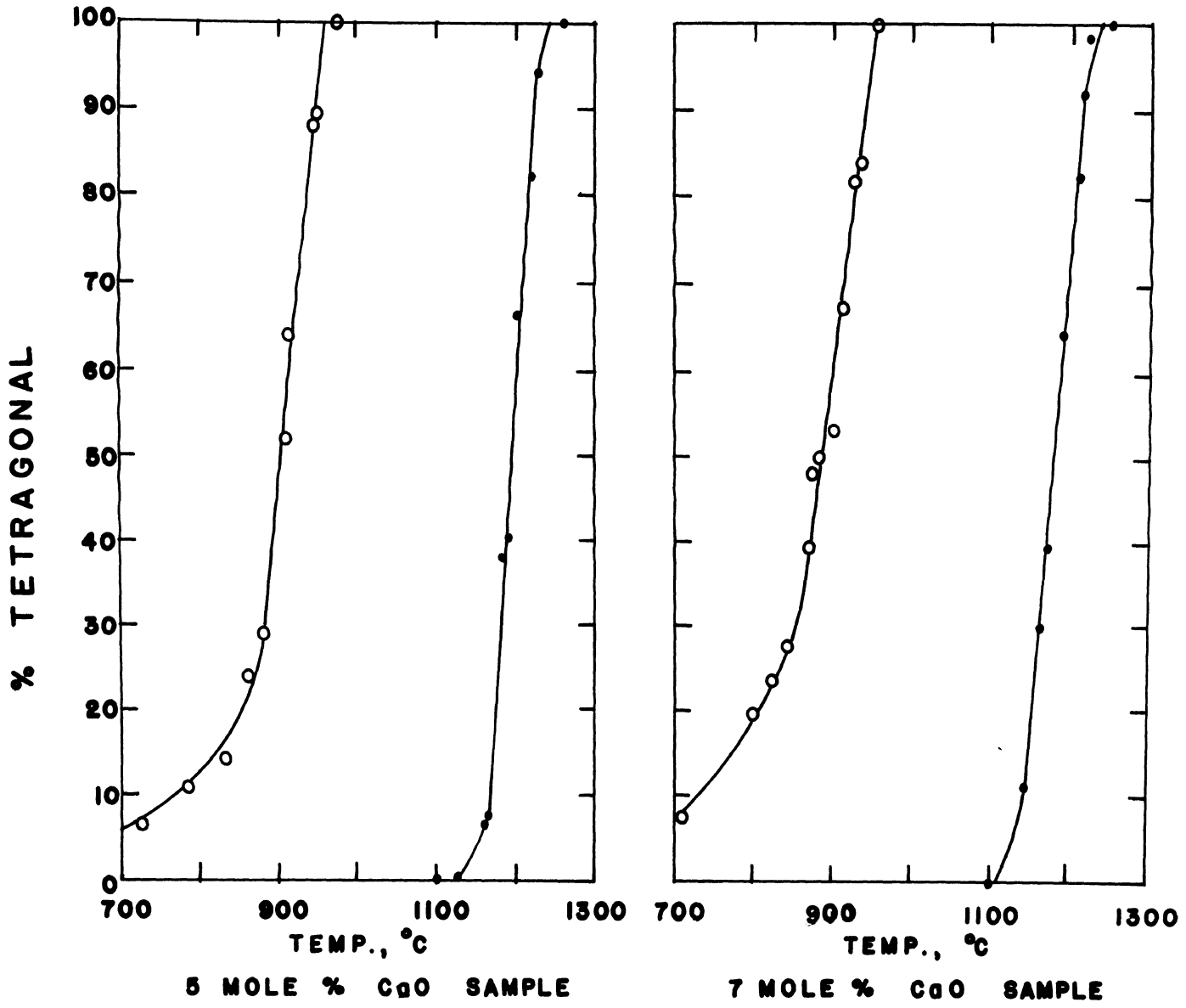
% TETRAGONAL
100
90
80
70
60
50
40
30
20
10
0
700
900
1100
1300
TEMP., °C
5 MOLE % CaO SAMPLE
700
900
1100
1300
TEMP., °C
7 MOLE % CaO SAMPLE

FIGURE 15

FIGURE 16

THERMAL HYSTERESIS LOOPS OF 10 MOLE % AND 12 MOLE % CaO SAMPLES.

Data obtained in same manner as for Figure 14.

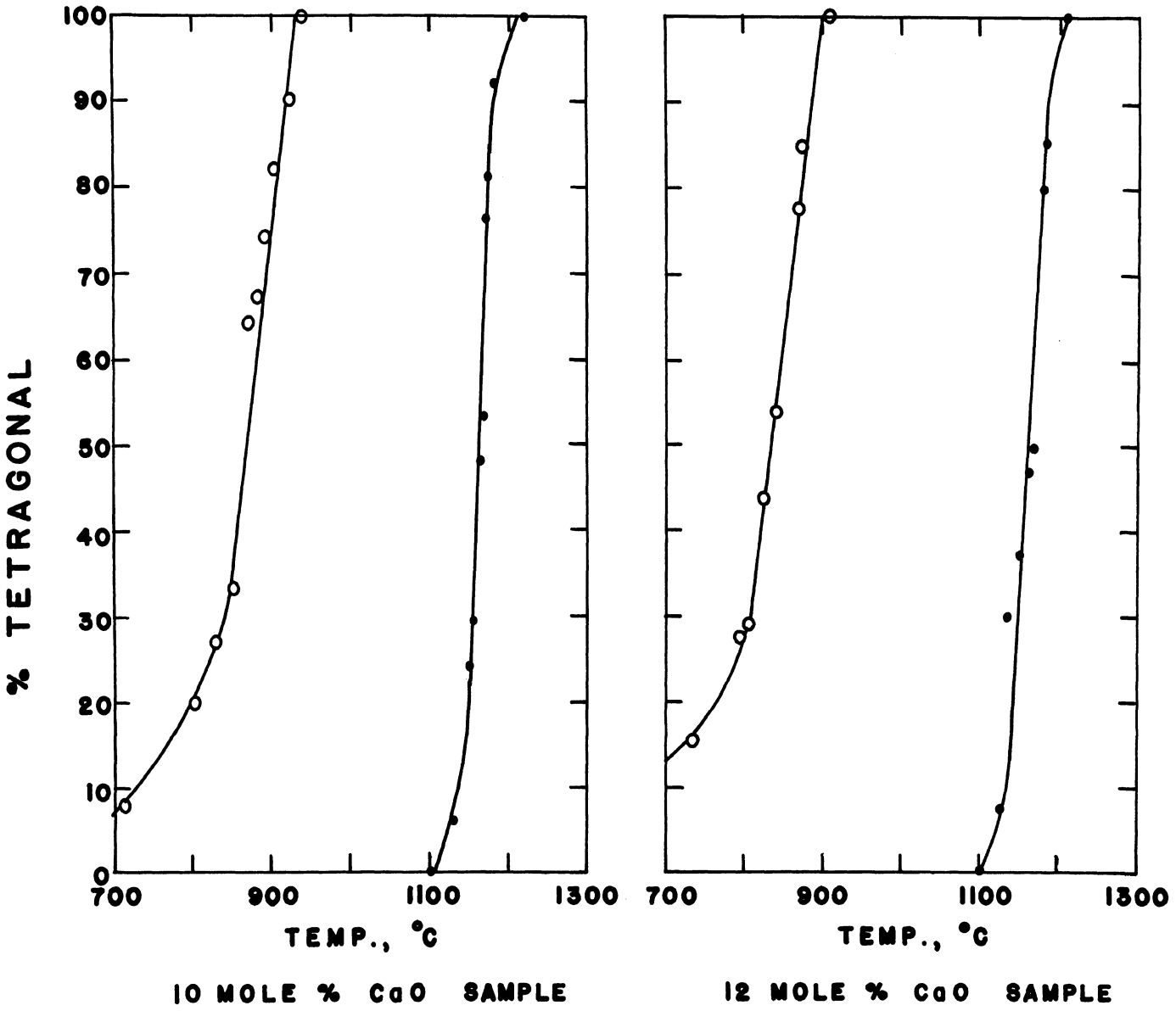
% TETRAGONAL
100
90
80
70
60
50
40
30
20
10
0
700
900
1100
1300
TEMP., °C
10 MOLE % CaO SAMPLE
700
900
1100
1300
TEMP., °C
12 MOLE % CaO SAMPLE

FIGURE 16

the monoclinic phase began to develop at about 1000°C and increased in amount with decreasing temperature . The increase of the monoclinic phase occurred very slowly below 900°C, and persisted to lower temperatures, producing a long tail in a hysteresis loop.

Further additions of CaO did not change the transformation temperature on heating appreciably, but retarded the reverse transformation. The transformation temperature on cooling decreased slightly with an increase in the content of CaO in the samples. With addition of 12 mole percent CaO, the transformation on cooling started at about 920°C and was complete at lower temperature, producing a long tail on the hysteresis loop. The width of the hysteresis loop increased with increasing CaO content.

The characteristics of the hysteresis loop depend on the thermal history of the samples. Figure 17 shows the hysteresis loops of a single composition preheated at different temperatures for different times. The transformation temperatures, on heating, are almost the same. Transformation started at about 1100°C and was complete at about 1250°C. The differences in the hysteresis loops are noted on the cooling portion. The hysteresis loop of the sample preheated at 1000°C for 200 hours exhibits the wider width of the loop.

C. Phase Relationships in the System ZrO_2-CaO

Heating and quenching techniques were used to determine

FIGURE 17

THERMAL HYSTERESIS LOOPS OF SAMPLES PREHEATED AT 1000°C AND 1400°C.

Data obtained in same manner as for Figure 14.

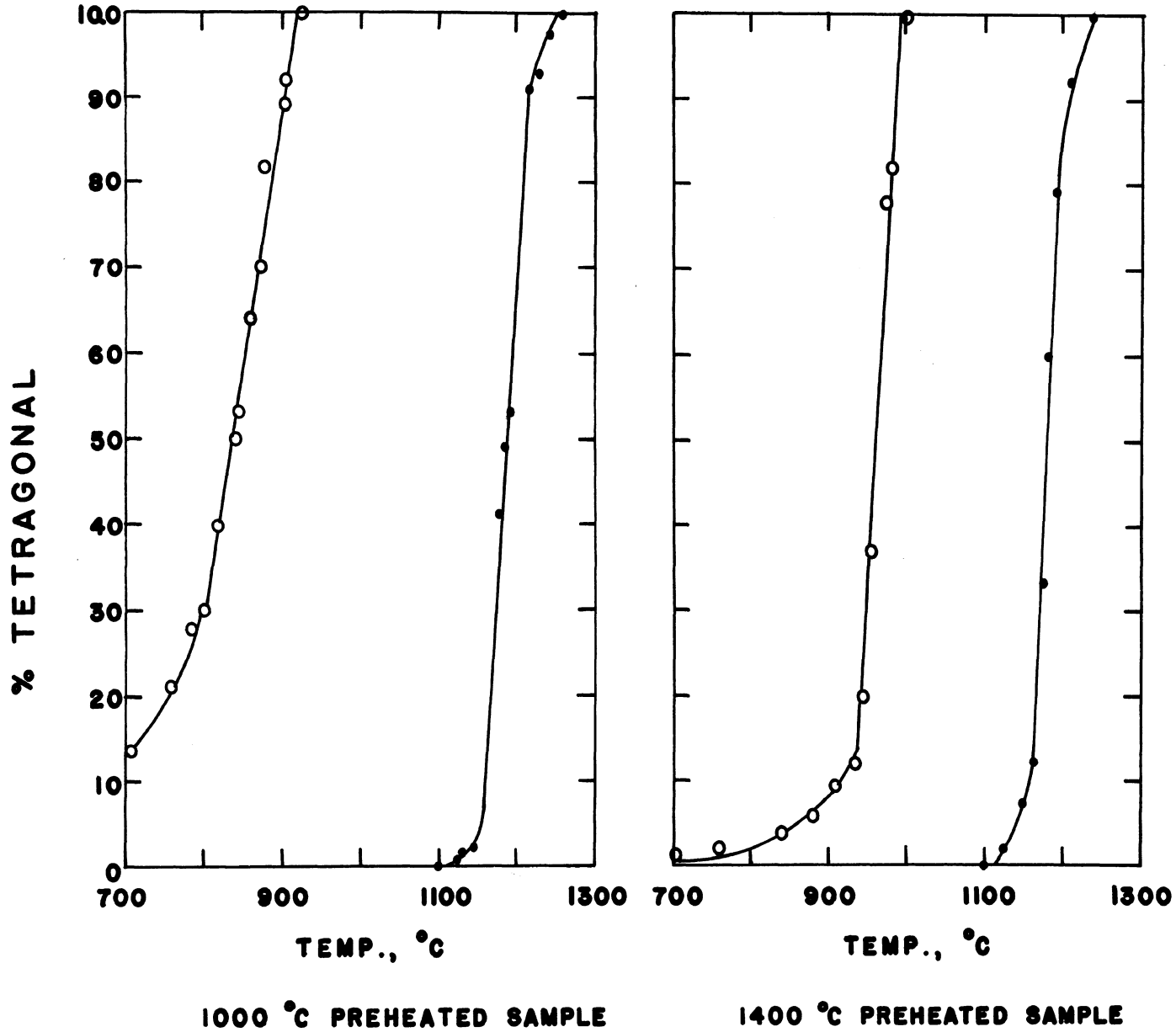
% TETRAGONAL
100
90
80
70
60
50
40
30
20
10
0
700
900
1100
1300
TEMP., °C
1000 °C PREHEATED SAMPLE
700
900
1100
1300
TEMP., °C
1400 °C PREHEATED SAMPLE

FIGURE 17

phase relationships in the ZrO_2-CaO system. After the samples were heated to equilibrium at the desired temperature, intensities and the lattice parameter were measured at room temperature. The phase field of the cubic solid solutions was considered to be the most important feature to be studied. Intensities of the cubic solid solution phases synthesized at all temperatures tabulated in Table IV. Figure 18 shows the percentages of the cubic solid solution phase at all temperatures as a function of the CaO content.

It can be seen that at higher temperatures the width of the cubic solid solution field is greater. The samples heated at 1010°C for 2500 hours were not at equilibrium, as indicated by the presence of three phases, monoclinic ZrO_2 phase, cubic solid solution, and $CaZrO_3$. Continued heat treatment at 1010°C, however, causes increased development of the cubic solid solution, with a concomitant decrease in $CaZrO_3$ content, indicating the ultimate equilibrium assemblange. The compositional range of the cubic solid solution at 1115°C is very narrow, approximately from 19% to 20% CaO. The ranges of the cubic field at 1250°, 1310°, 1400°, and 1500°C are 15 to 20 mole %, 14.5-20 mole %, 13.5-20 mole %, and 13-20 mole % CaO, respectively.

The lattice parameters of the cubic solid solutions at all temperatures are given in Table V and the plot of these data versus CaO content is shown in Figure 19. The lattice parameters of the cubic solid solution at any tem-

TABLE IV

Percentages of Cubic Solid Solution Phase

Sample No.	Temperature, °C 1115	1250	1310	1400	1500
1	0.00	0.00	0.00	0.00	0.00
2	-	3.76	2.04	2.08	6.06
3	-	9.11	9.00	10.24	-
4	-	13.49	18.81	20.60	-
5	-	27.48	35.98	32.78	-
6	-	41.44	47.12	47.74	53.01
7	-	61.68	69.62	71.68	76.55
8	61.05	76.77	85.69	89.91	88.61
9	71.08	92.17	96.52	100.00	100.00
10	80.55	100.00	100.00	100.00	-
11	86.98	100.00	100.00	100.00	100.00
12	94.31	100.00	100.00	100.00	-
112	100.00	96.53	97.10	97.01	100.00
13	93.09	87.60	91.81	91.49	-
14	-	75.75	78.96	82.67	-
15	-	71.41	72.63	72.92	-
16	-	59.17	62.20	58.56	-
17	-	46.04	47.95	45.23	-
18	-	27.34	26.35	32.10	-
19	-	18.14	11.27	14.36	-
20	-	0.00	0.00	0.00	-

FIGURE 18

PERCENTAGES OF CUBIC SOLID SOLUTION PHASES FOR ALL ISOTHERMS VERSUS CaO CONTENT.

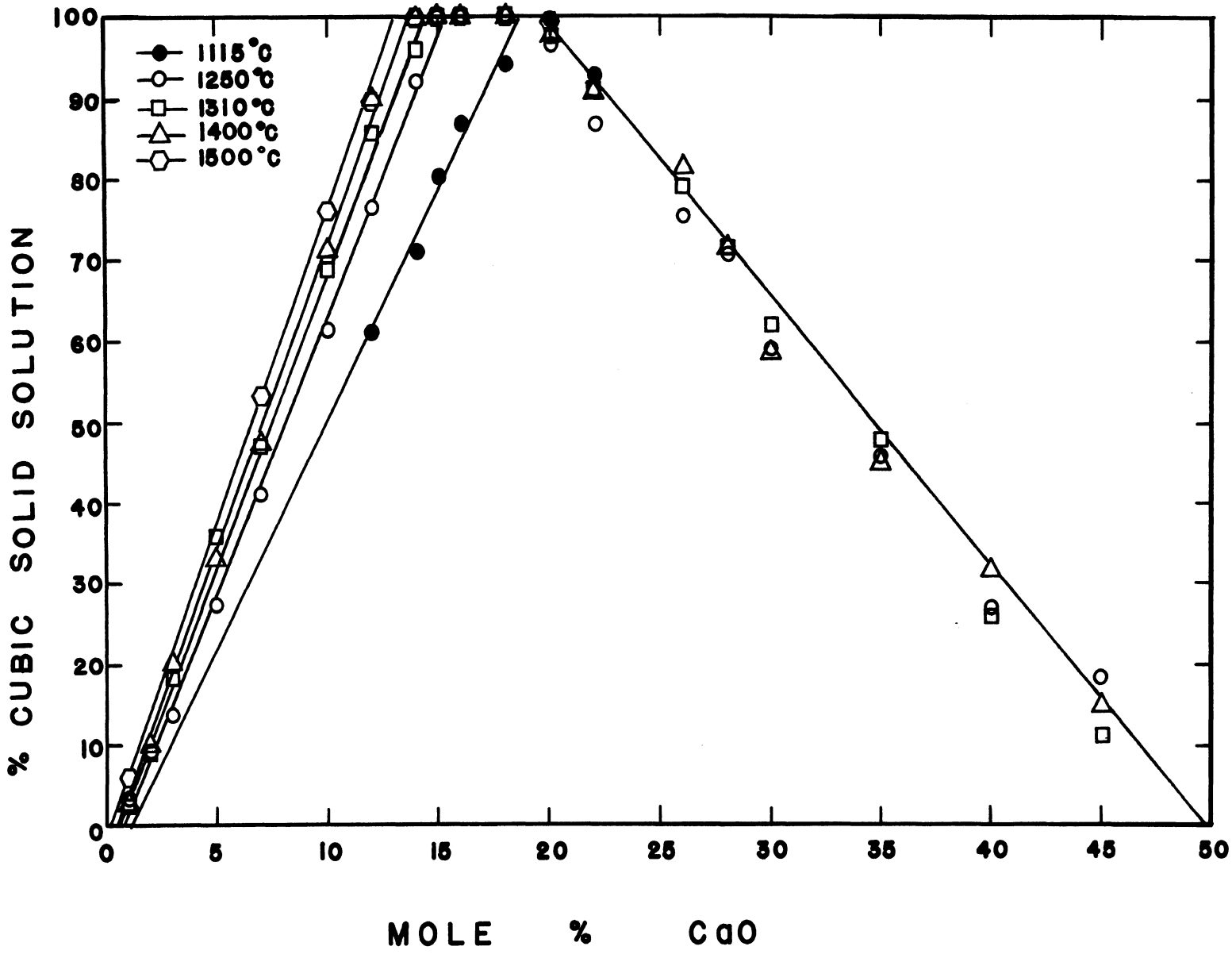
1115°C
1250°C
1310°C
1400°C
1500°C
% CUBIC SOLID SOLUTION
MOLE % CaO
0
10
20
30
40
50
60
70
80
90
100
0
5
10
15
20
25
30
35
40
45
50

FIGURE 18

TABLE V

Lattice Parameters of the Cubic Solid Solution

Composition (CaO mole %)	Preheated Temperature (°C) and Time (hrs.)				
	1115° 2542	1250° 325	1310° 175	1400° 100	1500° 40
10	-	5.1312	5.1288	5.1281	5.1277
12	5.1406	5.1303	5.1296	5.1275	5.1276
14	5.1406	5.1308	5.1292	5.1288	5.1300
15	5.1406	5.1305	5.1303	5.1305	-
16	5.1412	5.1327	5.1328	5.1328	5.1322
18	5.1406	5.1355	5.1375	5.1345	-
20	5.1420	5.1395	5.1405	5.1371	5.1390
22	5.1420	5.1404	5.1388	5.1388	5.1401
26	-	5.1404	5.1405	5.1388	-
28	-	5.1395	5.1405	5.1388	-

FIGURE 19

LATTICE PARAMETERS OF CUBIC SOLID SOLUTION PHASE VERSUS MOLE % CaO.

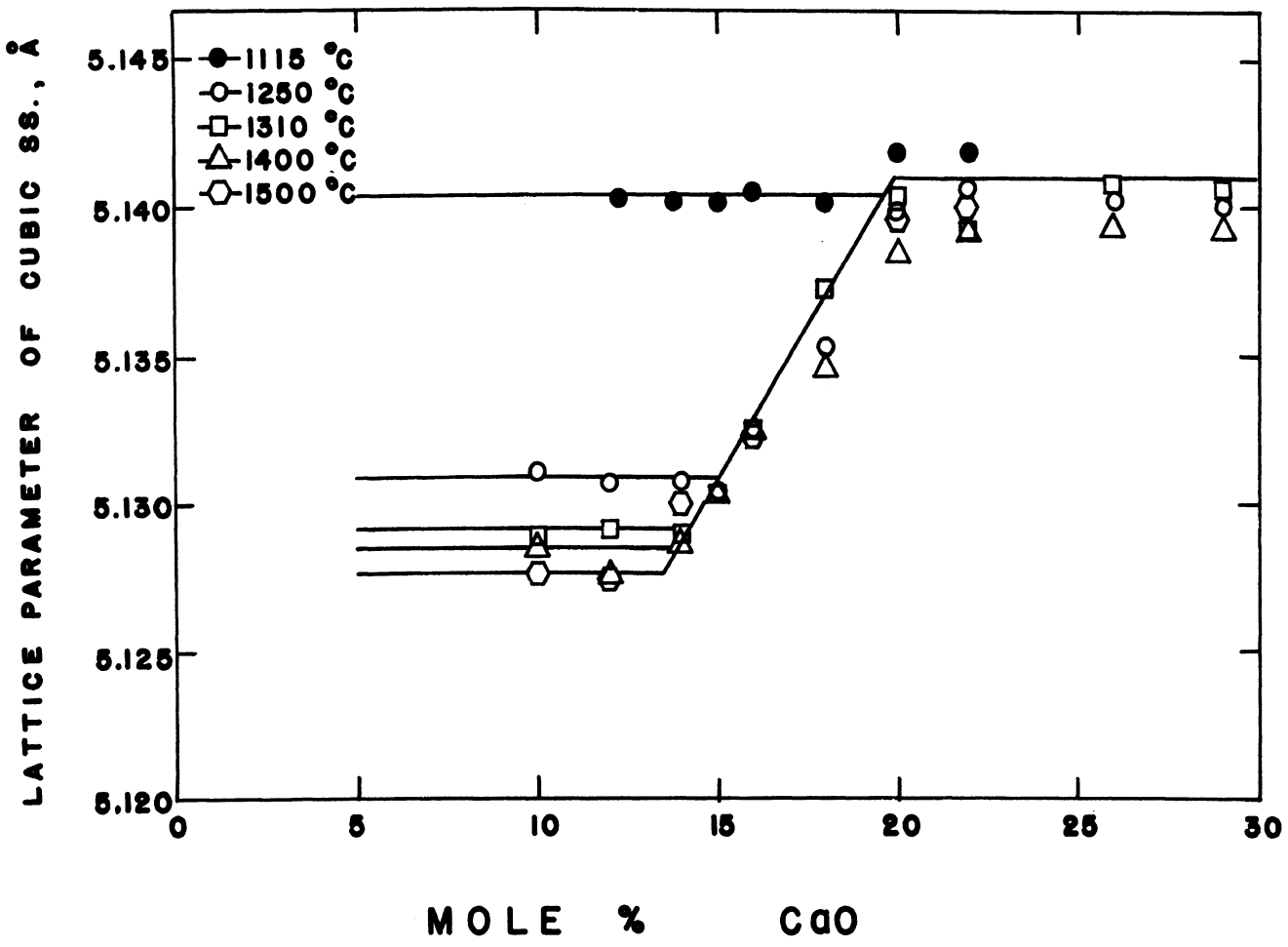
LATTICE PARAMETER OF CUBIC SS., Å
5.145
5.140
5.135
5.130
5.125
5.120
1115 °C
1250 °C
1310 °C
1400 °C
1500 °C
0
5
10
15
20
25
30
MOLE % CaO

FIGURE 19

perature is constant in the two phases region. In the region of the ZrO_2 plus cubic solid solution, at the left of the plot, the lattice parameter of the cubic solid solution decreases with increasing temperature. The lattice parameter in the solid solution range increases with increasing CaO content. In the cubic solid solution plus $CaZrO_3$ field the lattice parameter of the cubic solid solution is nearly constant with increasing temperature, with a boundary at about 20 mole % CaO.

The cubic field determined from lattice parameters is in close agreement with that determined from quantitative analyses of the cubic solid solution. The results agree quite closely with those of Garvie (Figure 6), though the present data indicate a slightly wider field.

High temperature x-ray techniques were used to determine the monoclinic $\rightleftarrows$ tetragonal phase transformation temperature of samples in the system ZrO_2-CaO. On heating, the transformation temperature seems to be reduced from 1150°C to 1100°C in the presence of a small amount of CaO in the ZrO_2. Further addition of CaO -- more than one mole percent -- to ZrO_2 did not reduce the transformation temperature further.

V. DISCUSSION AND CONCLUSIONS

A. The Monoclinic ⇄ Tetragonal Phase Transformation in ZrO_2

The thermal expansion results in this study are in good agreement with those of Campbell and Grain. They indicated no pre-transformation effects below the transformation. The lattice parameters before and after a heating and cooling cycle are not the same in samples not previously heated; larger parameters are observed after a heating and cooling cycle. This can probably be explained by formation of defects at higher temperatures and retention of defects on cooling.

Thermal expansion of the monoclinic form of ZrO_2 is highly anisotropic, with the lowest coefficient in the B_o direction and the highest in the C_o direction. The transformation can be discussed in terms of vibrational amplitudes, as indicated by thermal expansion. As the monoclinic form of ZrO_2 is heated, thermal vibrations in the A_o-C_o plane increase, with amplitudes greater in the C_o direction; vibrational amplitudes perpendicular to the plane, in the B_o direction are least. The observed coefficients of thermal expansion are consequences of the unique structure of monoclinic ZrO_2.

If the structures of the monoclinic and the tetragonal form of ZrO_2 are considered, it can be seen that the main difference is the stacking of the atoms on the A_o-C_o plane. The monoclinic B_o axis is parallel to the tetragonal C_o axis,

and this is correlated to the thermal expansion results. During the transformation, starting at about 1150°C, the rate of expansion seems to increase. This can be explained in terms of surface energy effects and the coherence of the planes with those of the tetragonal phase. The intensities of d_{002} and d_{020} of the monoclinic phase decrease and the intensity of d_{200} increases with increasing temperature in the transformation range. The d_{200} line of the monoclinic phase becomes the d_{110} line of the tetragonal phase. The d_{002} line of the tetragonal phase appears between the d_{002} and d_{020} lines of the monoclinic phase. These observations can be used to explain the mechanism of the monoclinic $\rightleftarrows$ tetragonal phase transformation in ZrO_2 as follows.

The monoclinic B_o axis is parallel to the tetragonal C_o axis. When the transformation starts, the monoclinic A_o axis expands until its dimension is about the same as that of B_o axis. This means that the atoms in the monoclinic structure are vibrating in the A_o-C_o plane and at the start of the transformation the positions of these atoms attain ordered positions, with zirconium atoms in eightfold coordination, corresponding to the tetragonal form. When the atoms are in ordered position they tend to decrease energy by decreasing the lattice parameters of the structure, thus the lattice parameters of the tetragonal structure are smaller than those of the monoclinic structure, even though they have the more open structure. At the transformation

temperature the tetragonal form has the lower free energy.

The tetragonal form is semicoherent with respect to the monoclinic form, so strain energy is produced. This energy brings the transformation reaction to a halt at any given temperature within the transformation range. For further transformation, the temperature must be increased. On cooling the reverse occurs. But, because the strain energy involved in accommodating a monoclinic phase in a tetragonal phase is not the same as the strain arising from a tetragonal phase in a monoclinic matrix phase; the hysteresis loop is produced. This can be explained either in terms of the martensitic transformation mechanism, as commented by several investigators,[16, 24] or Ubbelohde's theory, as discussed by Grain and Garvie.[13]

B. ZrO_2-CaO Phase Relationships

On addition of one mole % CaO to pure ZrO_2, the monoclinic-tetragonal phase transformation temperature is reduced from 1150° to 1100°C on heating, and on cooling the reverse transformation temperature is reduced from 1050° to 1000°C. With further addition of CaO to ZrO_2, the transformation on heating still starts at 1100°C, but the transformation temperature on cooling is lowered. The solid solubility limits in monoclinic and tetragonal ZrO_2 are, therefore, in the vicinity of one percent or less. Further additions of CaO result in development of the cubic solid solution. After the transformation of ZrO_2 is complete, the cubic solid solution can be coherent with the tetragonal

phase. On cooling, the cubic solid solution may have the effect of retarding formation of the monoclinic phase. With more cubic solid solution, the strain energy arising from coexistence of the cubic solid solution and tetragonal phases is greater. The higher content of CaO, therefore, lowers the transformation temperature on cooling and widens the hysteresis loop. On heating, the cubic solid solution phase has little effect on the monoclinic-tetragonal phase transformation.

The history of the samples has some effect on the transformation temperature and on transformation characteristics because of the differences in defect concentrations in the samples. The sample preheated at 1010°C for 200 hours exhibited the widest hysteresis loop. The explanation probably lies in the non-equilibrium conditions in the sample; there are many phases in the system -- monoclinic ZrO_2, cubic solid solution, a small amount of unreacted CaO, and a small amount of $CaZrO_3$. On heating, these phases have little effect on the monoclinic-tetragonal transformation. But on cooling, coexistence of these phases with the tetragonal phase has some effect on the reverse transformation, causing a lower transformation temperature. The samples preheated at higher temperatures will exhibit the narrower hysteresis loop due to defects, as discussed before.

The results from heated and quenched samples revealed that with higher preheating temperatures cubic solid solu-

tion range is wider. The data from this study are in good agreement with those of Garvie,[30] though this study indicates a slightly wider range of cubic solid solution. At reaction temperature, $CaCO_3$ gives off CO_2 gas and forms an active CaO, thereby providing a more rapid approach to equilibrium than CaO, as used by Garvie.

Lattice parameters for ZrO_2 with 20 mole percent or more CaO between 1115° to 1500°C do not vary with composition. Garvie[30] interpreted this to mean that a compound, $CaZr_4O_9$, is formed at 20 mole % CaO, and the cubic solid solution field is the result of solid solution of ZrO_2 in this compound. This interpretation seems reasonable if the cubic lattice parameter for equilibrium compositions in the vicinity of 20% CaO was constant at all temperatures but the upper phase boundary shifts to higher CaO contents with increasing temperature and x-ray data indicate no clear distinction between the cubic solid solutions and "$CaZr_4O_9$." Garvie indicated that there are two phases of $CaZr_4O_9$, alpha and beta,with a transformation temperature about 1650°C. The transformation has not as yet been verified by high-temperature x-ray study. Even if the lattice parameter data for the 20 mole percent or more CaO were constant with temperature, it does not necessarily mean that there is a compound formation. These data can be interpreted in terms of a vertical upper phase boundary for the cubic solid solution. The larger lattice parameters at the higher temperatures, 1700° and 1765°C, reveal that the phase

boundary line shifts.

One of the polymorphs of pure ZrO_2 is the cubic form, with the fluorite structure. The tetragonal form will transform to the cubic form at about 2370°C.[19] The x-ray pattern of the cubic solid solution phase in the system ZrO_2-CaO can also be interpreted in terms of a fluorite structure. Solid solution of CaO in ZrO_2 can be considered effective in lowering the tetragonal-cubic transformaion temperature to 1000°C at about 20% CaO. If the tetragonal-cubic transformation is induced by loss of O_2 and formation of a new phase, ZrO_{2-x}, solid solution of CaO in ZrO_2 would have an analogous effect, with formation of $Zr_{1-x}\ Ca_x\ O_{2-x}$, at lower temperatures.

Further support for existence of the cubic solid solution phase is the cubic solid solution forming in the system ZrO_2-MgO[37] as shown in Figure 20. MgO and CaO have the same crystal structure and similar properties. The difference in the cubic solid solution range is a result of the difference in the ionic radii of Mg^{+2} and Ca^{+2}. Figure 21 shows the phase diagram proposed for the system ZrO_2-CaO, based on the experimental work reported here.

FIGURE 20

ZrO_2-MgO PHASE DIAGRAM.

From C. F. Grain (1967).

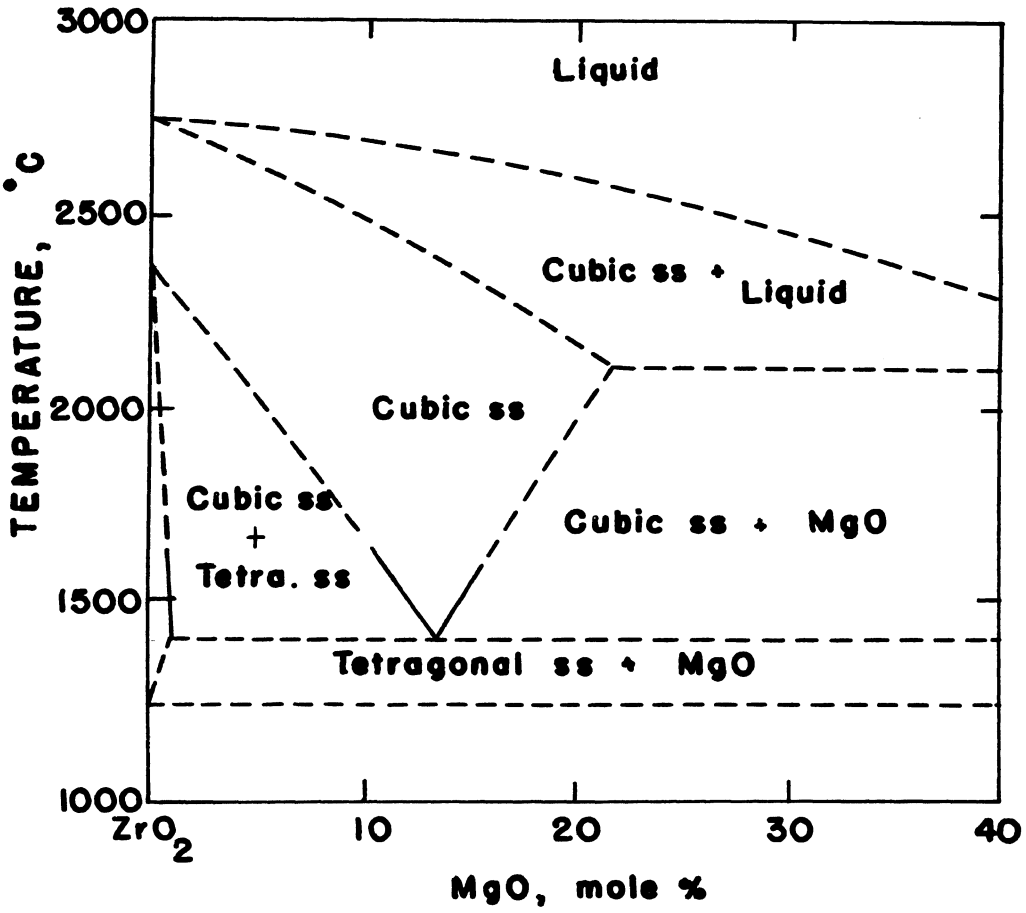
3000
2500
2000
1500
1000
TEMPERATURE, °C
Liquid
Cubic ss + Liquid
Cubic ss
Cubic ss + MgO
Cubic ss + Tetra. ss
Tetragonal ss + MgO
ZrO2
10
20
30
40
MgO, mole %

FIGURE 20

FIGURE 21

PROPOSED PHASE DIAGRAM OF THE SYSTEM ZrO_2-CaO.

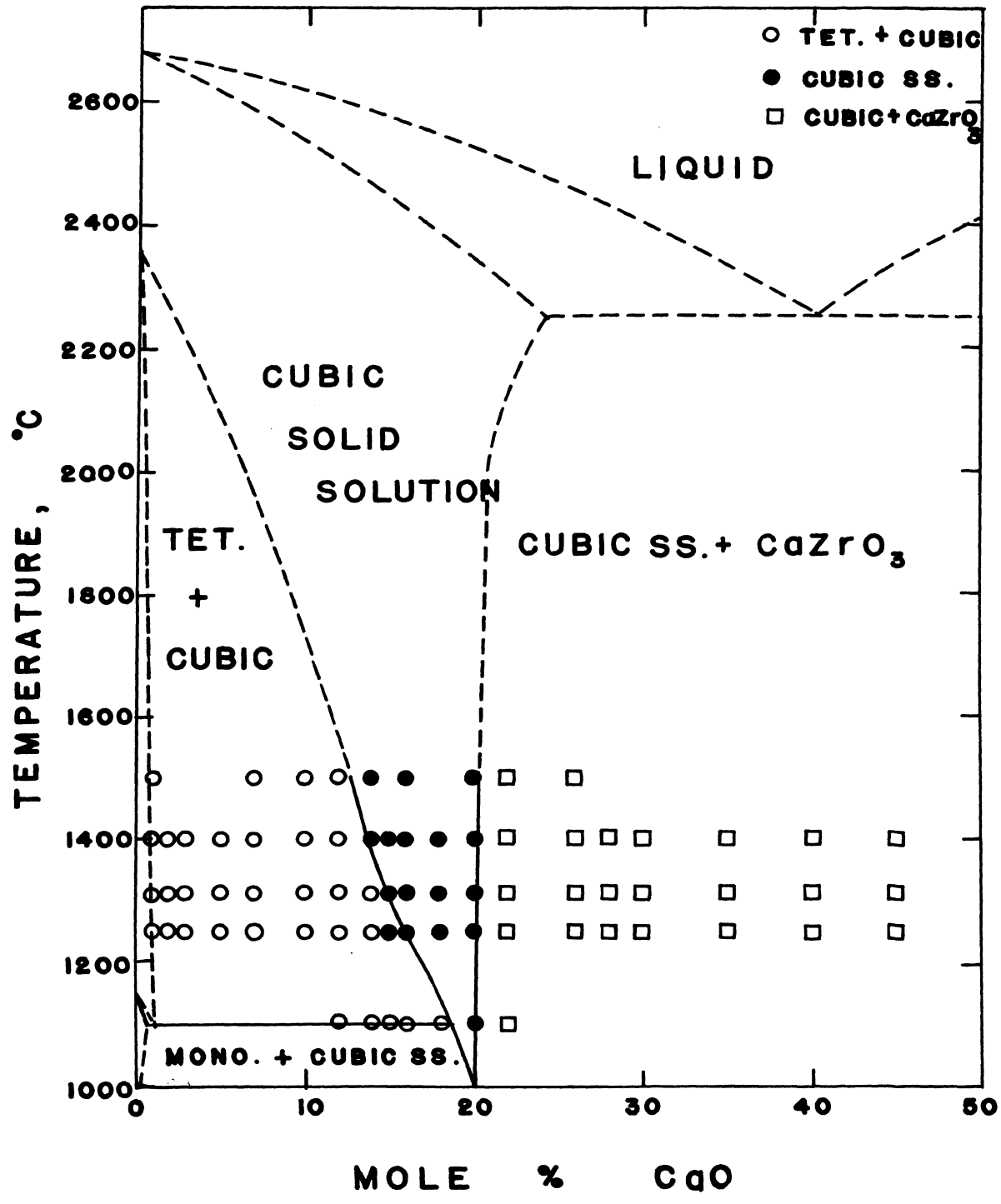
TET. + CUBIC
CUBIC SS.
CUBIC + CaZrO3
LIQUID
CUBIC
SOLID
SOLUTION
TET.
+
CUBIC
CUBIC SS. + CaZrO3
MONO. + CUBIC SS.
TEMPERATURE, °C
2600
2400
2200
2000
1800
1600
1400
1200
1000
0
10
20
30
40
50
MOLE % CaO

FIGURE 21

VI. APPENDICES

APPENDIX A

Thermal Expansion Data for ZrO_2

APPENDIX A

Thermal Expansion Data For ZrO_2

TABLE AI

Raw 2θ Data on Heating for the Monoclinic (M) and Tetragonal (T) Lines

Temp °C	2θ 111(M)	2θ 101(T)	2θ $11\bar{1}$(M)	2θ 002(M)	2θ 002(T)	2θ 020(M)	2θ 200(M), 110(T)
25	28.13	-	31.44	34.15	-	34.40	35.33
108	28.10	-	31.40	34.09	-	34.37	35.24
205	28.07	-	31.37	34.04	-	34.36	35.20
317	28.05	-	31.33	33.99	-	34.36	35.17
430	28.03	-	31.29	33.92	-	34.32	35.13
523	28.02	-	31.25	33.90	-	34.32	35.11
612	28.01	-	31.23	33.85	-	34.33	35.08
725	28.00	-	31.19	33.79	-	34.31	35.03
824	27.99	-	31.16	33.74	-	34.33	35.02
918	27.98	-	31.11	33.70	-	34.32	34.97
934	27.96	-	31.09	33.67	-	34.32	34.93

TABLE AI (Cont.)

Temp °C	2θ 111(M)	2θ 101(T)	2θ $11\bar{1}$(M)	2θ 002(M)	2θ 002(T)	2θ 020(M)	2θ 200(M), 110(T)
980	27.94	-	31.08	33.65	-	34.28	34.92
1016	27.96	-	31.06	33.62	-	34.31	34.92
1027	27.92	-	31.03	33.60	-	34.28	34.89
1083	27.92	-	31.02	33.57	-	34.28	34.87
1100	27.92	-	30.99	33.53	-	34.28	34.86
1117	27.92	-	31.00	33.53	-	34.28	34.85
1138	27.93	-	30.99	33.53	-	34.28	34.85
1155	27.93	-	30.99	33.53	-	34.30	34.84
1175	27.92	-	30.99	33.53	-	34.30	34.84
1188	27.91	-	30.98	33.50	-	34.28	34.82
1211	27.89	29.69	30.94	33.47	33.87	34.25	34.77
1216	27.89	29.70	30.95	33.50	33.91	34.31	34.81
1221	-	29.70	-	-	-	-	-
1243	27.88	29.66	30.90	33.45	33.84	34.26	34.73

TABLE AI (Cont.)

Temp °C	2θ 111(M)	2θ 101(T)	2θ $11\bar{1}$(M)	2θ 002(M)	2θ 002(T)	2θ 020(M)	2θ 200(M), 110(T)
1265	27.88	29.67	30.90	-	33.86	-	34.74
1290	-	29.65	-	-	33.82	-	34.74
1300	-	29.65	-	-	33.83	-	34.71
1320	-	29.62	-	-	33.79	-	34.70

TABLE AII

d-Spacing Data on Heating for the Monoclinic (M) and Tetragonal (T) Lines

Temp °C	d 111(M)	d 101(T)	d $11\bar{1}$(M)	d 002(M)	d 002(T)	d 020(M)	d 200(M), 110(T)
25	3.1721	-	2.8453	2.6254	-	2.6069	2.5404
108	3.1754	-	2.8488	2.6299	-	2.6091	2.5467
205	3.1787	-	2.8515	2.6337	-	2.6099	2.5495
317	3.1810	-	2.8550	2.6374	-	2.6099	2.5516
430	3.1832	-	2.8586	2.6427	-	2.6128	2.5544
523	3.1843	-	2.8621	2.6442	-	2.6128	2.5558
612	3.1854	-	2.8639	2.6480	-	2.6121	2.5579
725	3.1865	-	2.8675	2.6526	-	2.6136	2.5615
824	3.1876	-	2.8702	2.6564	-	2.6121	2.5622
918	3.1888	-	2.8747	2.6595	-	2.6128	2.5657
934	3.1910	-	2.8765	2.6618	-	2.6128	2.5686
980	3.1932	-	2.8774	2.6633	-	2.6158	2.5693
1016	3.1910	-	2.8792	2.6656	-	2.6136	2.5693

TABLE AII (Cont.)

Temp °C	d 111(M)	d 101(T)	d $\underline{111}$(M)	d 002(M)	d 002(T)	d 020(M)	d 200(M), 110(T)
1027	3.1955	-	2.8819	2.6671	-	2.6158	2.5714
1083	3.1955	-	2.8828	2.6695	-	2.6158	2.5729
1100	3.1955	-	2.8856	2.6726	-	2.6158	2.5736
1117	3.1955	-	2.8847	2.6726	-	2.6158	2.5743
1138	3.1943	-	2.8856	2.6726	-	2.6158	2.5743
1155	3.1943	-	2.8856	2.6726	-	2.6143	2.5750
1175	3.1955	-	2.8856	2.6726	-	2.6143	2.5750
1188	3.1966	-	2.8865	2.6749	-	2.6158	2.5764
1211	3.1988	3.0089	2.8901	2.6772	2.6465	2.6180	2.5800
1216	3.1988	3.0079	2.8892	2.6749	2.6435	2.6136	2.5772
1243	3.2000	3.0119	2.8938	2.6788	2.6488	2.6173	2.5829
1265	3.2000	3.0109	2.8938	-	2.6473	-	2.5822
1290	-	3.0128	-	-	2.6503	-	2.5822
1300	-	3.0128	-	-	2.6495	-	2.5844
1320	-	3.0158	-	-	2.6526	-	2.5851

TABLE AIII

Calculated Lattice Parameters for Monoclinic (M) and Tetragonal (T) ZrO_2

Based on Raw Data of Table AII

Temp °C	A_o (M)	B_o (M)	C_o (M)	β (M)	A_o (T)	C_o (T)
25	5.1477	5.2138	5.3200	99° 15'	-	-
108	5.1605	5.2182	5.3291	99° 15'	-	-
205	5.1662	5.2198	5.3368	99° 16'	-	-
317	5.1704	5.2198	5.3443	99° 15'	-	-
430	5.1756	5.2256	5.3545	99° 12'	-	-
523	5.1774	5.2256	5.3564	99° 9'	-	-
612	5.1806	5.2242	5.3630	99° 5'	-	-
725	5.1873	5.2272	5.3718	99° 2'	-	-
824	5.1882	5.2242	5.3790	99° 0'	-	-
918	5.1937	5.2256	5.3836	98° 54'	-	-
934	5.1998	5.2256	5.3884	98° 54'	-	-
980	5.2015	5.2316	5.3918	98° 56'	-	-

TABLE AIII (Cont.)

Temp °C	A_o (M)	B_o (M)	C_o (M)	β (M)	A_o (T)	C_o (T)
1016	5.2005	5.2272	5.3954	98° 50'	-	-
1027	5.2053	5.2316	5.3990	98° 52'	-	-
1083	5.2078	5.2316	5.4033	98° 51'	-	-
1100	5.2081	5.2316	5.4085	98° 47'	-	-
1117	5.2101	5.2316	5.4090	98° 48'	-	-
1138	5.2090	5.2316	5.4079	98° 44'	-	-
1155	5.2107	5.2286	5.4082	98° 45'	-	-
1175	5.2110	5.2286	5.4085	98° 46'	-	-
1188	5.2138	5.2316	5.4131	98° 47'	-	-
1211	5.2206	5.2360	5.4172	98° 44'	3.6487	5.2930
1216	5.2151	5.2272	5.4128	98° 45'	3.6447	5.2870
1243	5.2248	5.2346	5.4188	98° 38'	3.6528	5.2976
1265	-	-	-	-	3.6518	5.2946
1290	-	-	-	-	3.6518	5.3006

TABLE AIII (Cont.)

Temp °C	A_o (M)	B_o (M)	C_o (M)	β (M)	A_o (T)	C_o (T)
1300	-	-	-	-	3.6549	5.2990
1320	-	-	-	-	3.6559	5.3052

TABLE AIV

Raw 2θ Data on Cooling for Monoclinic (M) and Tetragonal (T)

X-Ray Powder Lines

Temp °C	2θ 111(M)	2θ 101(T)	2θ 111(M)	2θ 002(M)	2θ 002(T)	2θ 020(M)	2θ 200(M), 110(T)
1216	-	29.66	-	-	33.86	-	34.73
1144	-	29.76	-	-	33.95	-	34.83
1087	-	29.79	-	-	33.98	-	34.88
1083	-	29.78	-	-	33.99	-	34.85
1040	-	29.80	-	-	34.01	-	34.87
1023	-	29.79	-	-	-	-	34.86
992	27.92	29.80	31.07	33.64	-	-	34.89
986	27.92	29.78	31.04	33.60	34.00	34.30	34.88
961	27.96	29.82	31.07	33.63	-	34.33	34.92
926	27.94	29.80	31.06	33.63	-	34.30	34.90
916	27.98	29.85	31.14	33.70	-	-	34.98
896	27.93	29.82	31.07	33.68	-	34.28	34.96

TABLE AIV (Cont.)

Temp °C	2θ 111(M)	2θ 101(T)	2θ 111(M)	2θ 002(M)	2θ 002(T)	2θ 020(M)	2θ 200(M), 110(T)
862	27.95	29.86	31.11	33.71	-	34.31	34.98
801	27.95	29.86	31.12	33.71	-	34.30	34.96
765	27.98	-	31.15	33.76	-	34.31	34.99
600	27.97	-	31.19	33.80	-	34.30	35.03
315	28.04	-	31.30	33.95	-	34.32	35.13
236	28.04	-	31.33	34.00	-	34.36	35.17
108	28.06	-	31.37	34.03	-	34.34	35.19
25	28.08	-	31.39	34.08	-	34.35	35.22

TABLE AV

d-Spacing Data on Cooling for the Monoclinic (M) and Tetragonal (T)

X-Ray Powder Lines

Temp °C	d 111(M)	d 101(T)	d $11\bar{1}$(M)	d 002(M)	d 002(T)	d 020(M)	d 200(M), 110(T)
1216	-	3.0119	-	-	2.6473	-	2.5829
1144	-	3.0020	-	-	2.6404	-	2.5757
1087	-	2.9990	-	-	2.6382	-	2.5721
1083	-	3.0000	-	-	2.6374	-	2.5743
1040	-	2.9980	-	-	2.6359	-	2.5729
1023	-	2.9990	-	-	2.6359	-	2.5736
992	3.1955	2.9980	2.8783	2.6641	-	-	2.5714
986	3.1955	3.0000	2.8810	2.6671	2.6367	2.6143	2.5721
961	3.1910	2.9961	2.8783	2.6648	-	2.6121	2.5693
926	3.1932	2.9980	2.8792	2.6648	-	2.6143	2.5707
916	3.1888	2.9931	2.8720	2.6595	-	-	2.5650
896	3.1943	2.9961	2.8783	2.6610	-	2.6158	2.5664

TABLE AV (Cont.)

Temp °C	d 111(M)	d 101(T)	d $11\bar{1}$(M)	d 002(M)	d 002(T)	d 020(M)	d 200(M), 110(T)
862	3.1921	2.9921	2.8747	2.6587	-	2.6136	2.5650
801	3.1921	2.9921	2.8738	2.6587	-	2.6143	2.5664
765	3.1888	-	2.8711	2.6549	-	2.6136	2.5643
600	3.1899	-	2.8675	2.6518	-	2.6143	2.5615
315	3.1821	-	2.8577	2.6404	-	2.6128	2.5544
236	3.1821	-	2.8550	2.6367	-	2.6099	2.5516
108	3.1798	-	2.8515	2.6344	-	2.6113	2.5502
25	3.1776	-	2.8497	2.6307	-	2.6106	2.5481

TABLE AVI

Calculated Lattice Parameters for Monoclinic (M) and Tetragonal (T) ZrO_2

Based on Raw Data of Table AV

Temp °C	A_o (M)	B_o (M)	C_o (M)	β (M)	A_o (T)	C_o (T)
1216	-	-	-	-	3.6528	5.2946
1144	-	-	-	-	3.6426	5.2808
1087	-	-	-	-	3.6375	5.2764
1083	-	-	-	-	3.6406	5.2748
1040	-	-	-	-	3.6386	5.2718
1023	-	-	-	-	3.6396	5.2718
992	5.2068	-	5.3946	98° 59'	3.6365	-
986	5.2067	5.2286	5.3990	98° 54'	3.6375	5.2734
961	5.2010	5.2242	5.3943	98° 52'	3.6335	-
926	5.2038	5.2286	5.3943	98° 53'	3.6355	-
916	5.1939	-	5.3852	98° 59'	3.6275	-
896	5.1957	5.2316	5.3872	98° 55'	-	-

TABLE AVI (Cont.)

Temp °C	A_o (M)	B_o (M)	C_o (M)	β (M)	A_o (T)	C_o (T)
862	5.1934	5.2272	5.3831	98° 58'	-	-
801	5.1967	5.2286	5.3836	99° 0'	-	-
765	5.1925	5.2272	5.3759	99° 0'	-	-
600	5.1884	5.2286	5.3713	99° 7'	-	-
315	5.1756	5.2256	5.3498	99° 12'	-	-
236	5.1704	5.2198	5.3429	99° 16'	-	-
108	5.1686	5.2226	5.3393	99° 19'	-	-
25	5.1638	5.2212	5.3312	99° 18'	-	-

APPENDIX B

X-Ray Patterns of Pure ZrO_2 at Different Temperatures, and of Phases in the System ZrO_2-CaO

High-temperature x-ray data for pure ZrO_2 and x-ray data obtained at room temperature for phases in the system ZrO_2-CaO, preheated at 1400°C for 100 hours, are contained in this appendix.

High-temperature x-ray techniques were used to measure thermal expansion and to study the monoclinic-tetragonal transformation of ZrO_2.

FIGURE B1

HIGH TEMPERATURE X-RAY DIFFRACTION DATA AT SELECTED TEMPERATURES ON HEATING OF PURE ZrO_2.

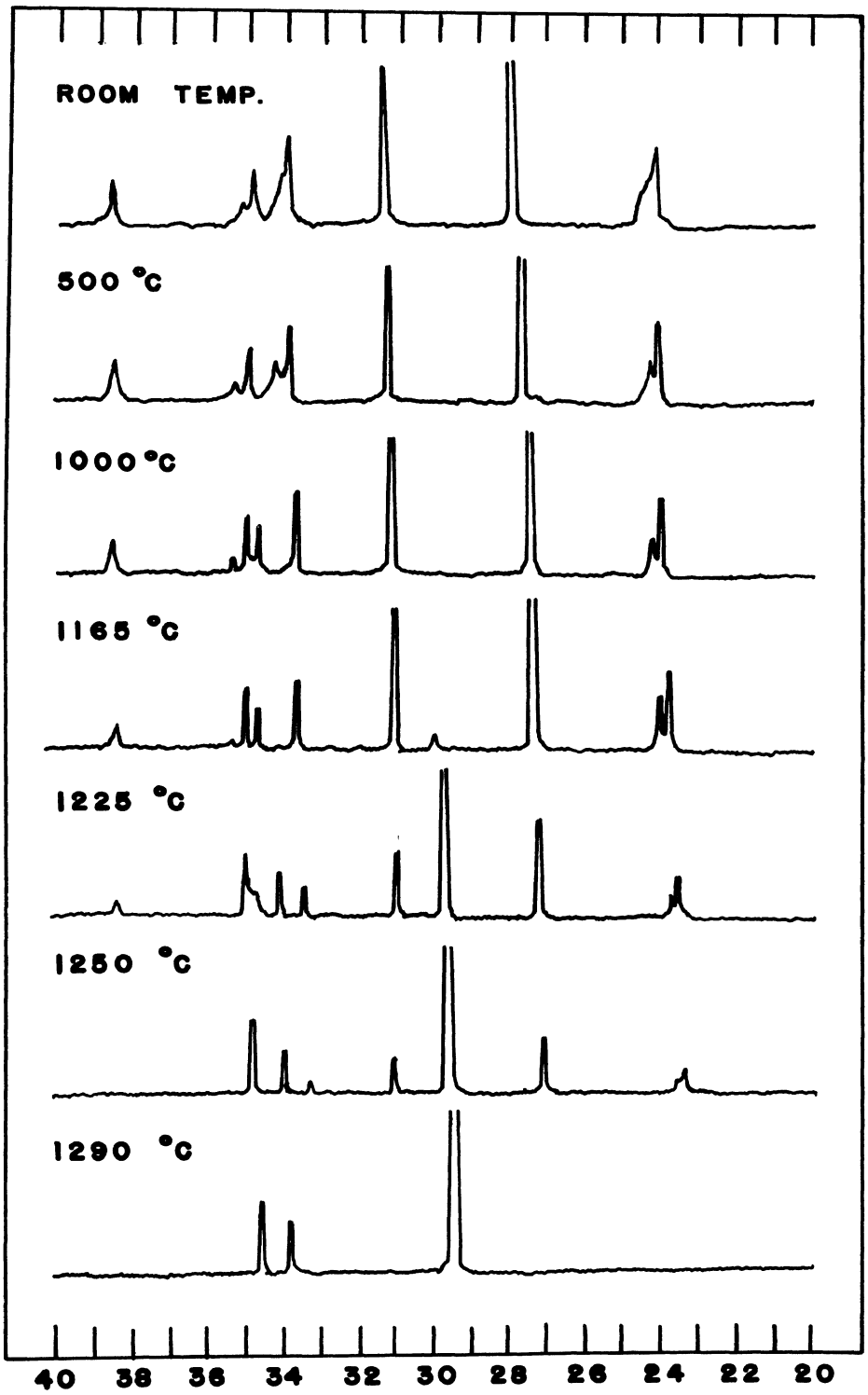
ROOM TEMP.
500 °C
1000 °C
1165 °C
1225 °C
1250 °C
1290 °C
40 38 36 34 32 30 28 26 24 22 20
DEGREES 2θ

FIGURE B1

FIGURE B2

HIGH TEMPERATURE X-RAY DIFFRACTION DATA AT SELECTED TEMPERATURES ON COOLING OF PURE ZrO_2.

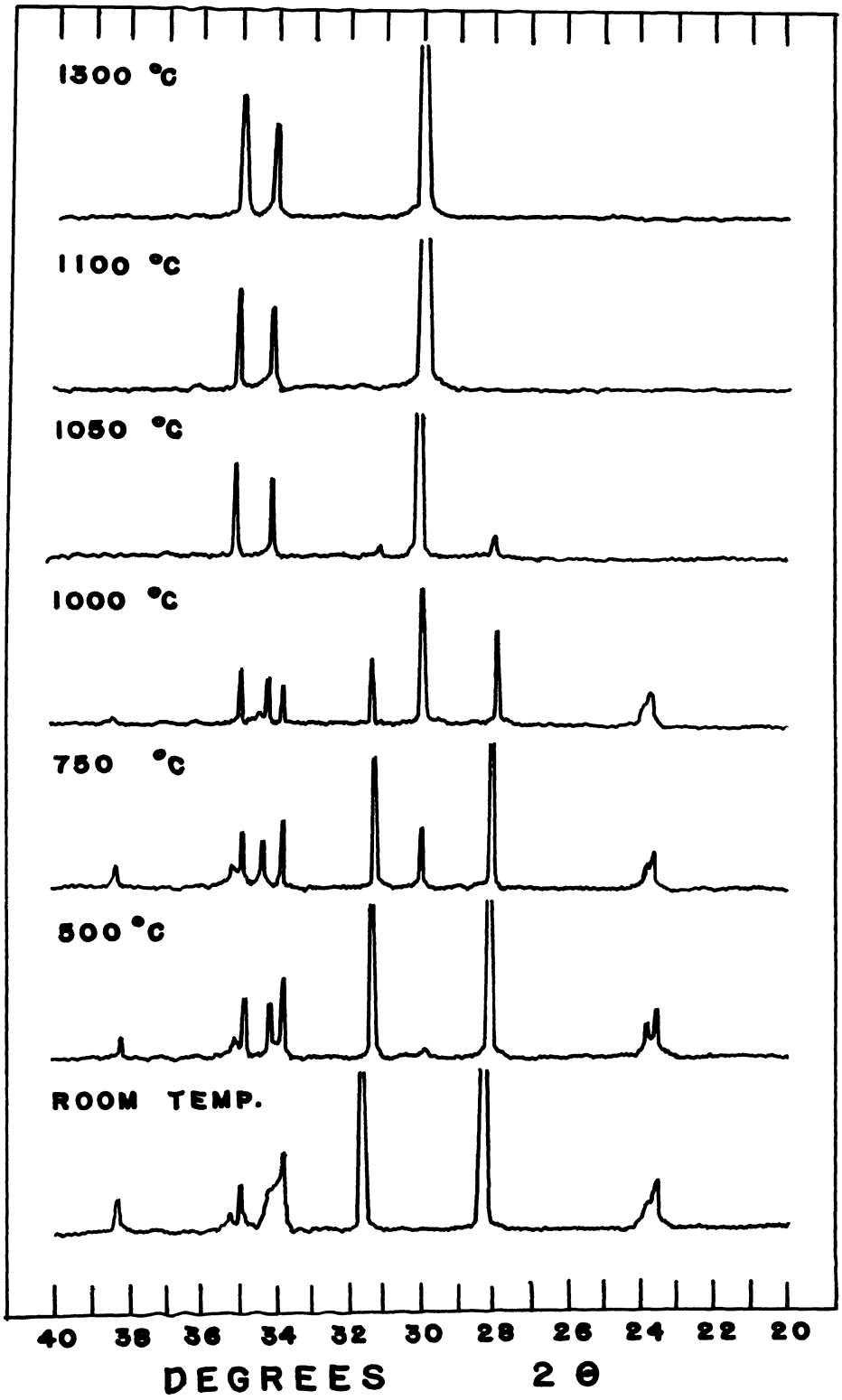
1300 °C
1100 °C
1050 °C
1000 °C
750 °C
500 °C
ROOM TEMP.
40 38 36 34 32 30 28 26 24 22 20
DEGREES 2θ

FIGURE B2

FIGURE B3

X-RAY DIFFRACTION PATTERNS OF PHASES IN THE SYSTEM ZrO_2-CaO.

The samples were heated at 1400°C for 100 hours and scanned at room temperature. X-ray patterns of monoclinic ZrO_2, the cubic solid solution, and $CaZrO_3$ are shown in this figure.

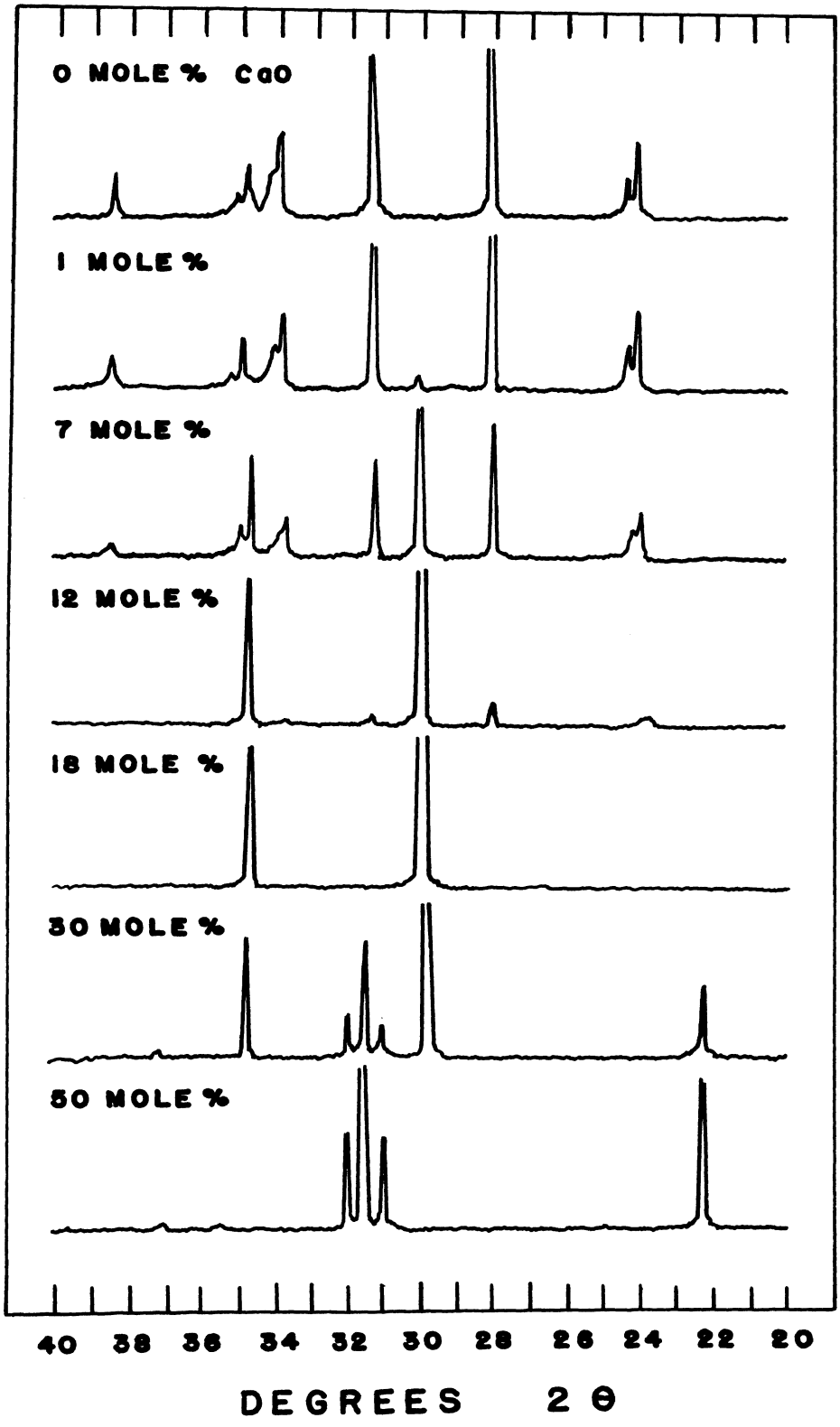
0 MOLE % CaO
1 MOLE %
7 MOLE %
12 MOLE %
18 MOLE %
30 MOLE %
50 MOLE %
40 38 36 34 32 30 28 26 24 22 20
DEGREES 2 θ

FIGURE B3

APPENDIX C

Original Data for Hysteresis Loops

The tables included in this appendix contain values of calculated percentages of tetragonal phase, developed over the transformation range, in pure ZrO_2 and ZrO_2-CaO. Preliminary heating time of each sample is indicated. All of the data are based on high-temperature x-ray diffraction measurements.

TABLE CI

Percentages of Tetragonal Phase Observed During Heating and Cooling of a Sample of ZrO_2 Not Previously Heated

Heating Temp.	% Tetragonal Phase	Cooling Temp.	% Tetragonal Phase
1140	0.00	1055	100.00
1153	2.40	1049	97.18
1180	2.03	1042	88.90
1186	2.52	1038	86.47
1187	3.81	1026	53.50
1205	7.67	995	28.36
1224	52.94	964	16.85
1246	77.84	925	10.43
1250	92.24	900	9.30
1268	95.98	880	7.51
1280	95.44	825	6.22
1290	99.79	770	4.54
1301	99.81	710	3.85

TABLE CII

Percentages of Tetragonal Phase Observed During Heating and Cooling of a Sample Preheated at 1400°C for 100 hours

Heating Temp.	% Tetragonal Phase	Cooling Temp.	% Tetragonal Phase
1140	0.00	1100	100.00
1158	1.34	1082	97.13
1172	1.68	1077	94.05
1176	2.81	1065	87.67
1185	3.16	1055	69.51
1196	8.93	1040	54.45
1209	28.26	1030	35.52
1215	46.04	—	—
1228	86.64	995	22.08
1241	89.71	964	12.86
1250	95.89	929	14.93
1255	99.74	901	11.24
1273	99.84	—	—
1283	100.00	862	9.87
		752	5.32
		726	5.01

TABLE CIII

Percentages of the Tetragonal Phase During Heating and Cooling of the 1 mole % CaO Sample Preheated at 1250°C for 325 hours

Heating Temp.	% Tetragonal Phase	Cooling Temp.	% Tetragonal Phase
1116	0.55	1000	100.00
1123	0.63	984	93.68
1142	2.25	980	88.76
1160	5.68	960	68.44
1166	8.70	946	52.42
1170	12.09	940	52.08
1176	13.17	938	44.12
1193	54.56	903	19.44
1202	82.93	880	15.39
1211	85.76	847	12.47
1232	96.60	827	8.90
1236	98.08	797	8.62
1250	100.00	741	4.86

TABLE CIV

Percentages of the Tetragonal Phase During Heating and Cooling of the 2 mole % CaO Sample Preheated at 1250°C for 325 hours

Heating Temp.	% Tetragonal Phase	Cooling Temp.	% Tetragonal Phase
1100	0.00	1000	100.00
1121	1.32	972	81.05
1144	3.50	959	75.03
1150	4.02	938	50.85
1178	20.35	916	28.20
1180	21.46	898	23.28
1187	32.83	860	18.26
1196	40.04	852	13.51
1203	73.66	842	11.92
1221	82.17	783	8.31
1235	98.91	700	6.50
1250	100.00		

TABLE CV

Percentages of the Tetragonal Phase During Heating and Cooling of the 5 mole % CaO Sample Preheated at 1250°C for 325 hours

Heating Temp.	% Tetragonal Phase	Cooling Temp.	% Tetragonal Phase
1100	0.00	975	100.00
1125	0.23	951	89.28
1160	6.30	944	88.75
1166	6.74	916	64.96
1182	38.10	911	52.71
1192	40.06	882	29.20
1202	66.26	862	24.32
1220	82.27	831	14.77
1230	94.15	785	10.82
1260	100.00	735	6.12

TABLE CVI

Percentages of the Tetragonal Phase During Heating and Cooling of the 7 mole % CaO Sample Preheated at 1250°C for 325 hours

Heating Temp.	% Tetragonal Phase	Cooling Temp.	% Tetragonal Phase
1100	0.00	955	100.00
1148	11.22	934	84.29
1165	30.04	927	82.41
1172	38.96	911	67.42
1192	64.13	900	53.77
1211	82.64	884	50.84
1216	92.35	876	48.97
1223	98.02	870	39.42
1250	100.00	840	28.28
		824	24.53
		800	20.03
		710	8.25

TABLE CVII

Percentages of the Tetragonal Phase During Heating and Cooling of the 10 mole % CaO Sample Preheated at 1250°C for 325 hours

Heating Temp.	% Tetragonal Phase	Cooling Temp.	% Tetragonal Phase
1100	0.00	940	100.00
1130	6.21	922	90.67
1150	24.51	903	82.86
1154	29.50	890	74.69
1165	48.01	880	67.37
1169	53.76	869	64.11
1172	76.26	853	33.65
1176	81.96	830	27.41
1180	92.39	806	20.02
1220	100.00	712	8.07

TABLE CVIII

Percentages of the Tetragonal Phase During Heating and Cooling of the 12 mole % CaO Sample Preheated at 1250°C for 325 hours

Heating Temp.	% Tetragonal Phase	Cooling Temp.	% Tetragonal Phase
1100	0.00	910	100.00
1125	7.32	876	85.70
1135	30.15	870	78.36
1150	37.55	842	54.02
1165	46.88	825	44.38
1169	49.61	806	29.02
1180	80.28	790	28.11
1186	85.21	738	16.17
1210	100.00		

TABLE CIX

Percentages of the Tetragonal Phase During Heating and Cooling of the 1 mole % CaO Sample Preheated at 1000°C for 200 hours

Heating Temp.	% Tetragonal Phase	Cooling Temp.	% Tetragonal Phase
1100	0.00	925	100.00
1122	0.50	905	92.40
1130	1.52	901	89.71
1154	1.85	876	82.19
1179	41.87	870	70.28
1185	47.78	859	64.61
1197	53.46	844	53.48
1215	90.68	839	51.14
1231	92.71	815	39.79
1247	98.69	800	30.51
1260	100.00	785	28.00
		760	20.96
		704	13.46

TABLE CX

Percentages of the Tetragonal Phase During Heating and Cooling of the 1 mole % CaO Sample Preheated at 1400°C for 100 hours

Heating Temp.	% Tetragonal Phase	Cooling Temp.	% Tetragonal Phase
1100	0.00	1000	100.00
1127	2.35	980	82.29
1150	7.21	972	78.54
1164	12.78	958	37.93
1175	32.88	941	20.32
1180	60.39	932	12.05
1192	79.45	910	10.41
1210	92.51	880	6.31
1230	100.00	843	4.64
		760	3.25
		700	1.70

VII. BIBLIOGRAPHY

1. K. Yardley, "The Structure of Baddeleyite and of Prepared Zirconia," Mineral Mag., 21, 169 (1926).

2. O. Ruff and F. Ebert, "Ceramics of Highly Refractory Materials. I. Forms of Zirconium Dioxide," Z. Anorg. Chem., 180, 19-41 (1929); Ceram. Abstr., 8 (9) 660 (1929).

3. W. M. Cohn and S. Tolksdorf, "Form of Zircon Dioxide Depending on the Treatment," Z. Phys. Chem., 8 (5) 331-56 (1930); Ceram. Abstr., 10 (8) 604 (1931).

4. S. V. Naray-Szabo, "The Structure of Baddeleyite, ZrO_2," Z. Krist., 94A, 414 (1936).

5. P. Duwez and F. Odell, "Phase Relationships in the System Zirconia-Ceria," J. Am. Ceram. Soc., 33 (9) 274-83 (1950).

6. J. D. McCullough and K. N. Trueblood, "The Crystal Structure of Baddeleyite (Monoclinic ZrO_2)," Acta Cryst., 12, 507-11 (1959).

7. D. K. Smith and H. W. Newkirk, "The Crystal Structure of Baddeleyite (Monoclinic ZrO_2) and its Relation to the Polymorphism of ZrO_2," Acta Cryst., 18, 983-91 (1965).

8. O. Ruff, F. Ebert, and E. Stephan, "Contributions to the Ceramics of Highly Refractory Materials. II. The System: Zirconia-Lime," Z. Anorg. Allgem. Chem., 180, 215-24 (1929); Ceram. Abstr., 8 (9) 749 (1929).

9. G. Teufer, "The Crystal Structure of Tetragonal ZrO_2," Acta Cryst., 15, 1187 (1962).

10. G. L. Clark and D. H. Reynolds, "Chemistry of Zirconium Dioxide. X-Ray Diffraction Studies," Ind. Eng. Chem., 29 (6) 711-15 (1937); Ceram. Abstr., 16 (8) 259 (1937).

11. K. S. Mazdiyasni, C. T. Lynch, and J. S. Smith, "Metastable Transitions of Zirconium Oxide Obtained from Decomposition of Alkoxides," J. Am. Ceram. Soc., 49 (5) 286-87 (1966).

12. R. Cypres, R. Wollast, and J. Raucq, "Polymorphic Transformations of Pure Zirconia," Ber. Deut. Keram. Ges., 40, 527 (1963).

13. R. C. Garvie, "Zirconium Dioxide and Some of Its Binary Systems," p. 117-66 in High Temperature Oxides, A. M. Alper (Ed.), Academic Press, New York, (1971).

14. D. K. Smith and C. F. Cline, "Verification of Existence of Cubic Zirconia at High Temperature," J. Am. Ceram. Soc., 45 (5) 249-50 (1962).

15. B. C. Weber, "Inconsistencies in Zirconia Literature," J. Am. Ceram. Soc., 45 (12) 614-15 (1962).

16. G. M. Wolten, "Diffusionless Phase Transformations in Zirconia and Hafnia," J. Am. Ceram. Soc., 46 (9) 418-22 (1963).

17. A. G. Boganov, V. S. Rudenko, and L. P. Makarov, "X-Ray Investigation of Zirconium and Hafnium Dioxides at Temperatures up to 2750°C," Dokl. Akad. Nauk SSSR, 160 (5) 1065-68 (1965).

18. R. Ruh and T. J. Rockett, "Proposed Phase Diagram for the System ZrO_2," J. Am. Ceram. Soc., 53 (6) 360 (1970).

19. P. S. Nicholson, "Influence of Reduction on Estimation of the ZrO_2 Tetragonal-Cubic Transformation Temperature," J. Am. Ceram. Soc., 54 (1) 52-53 (1971).

20. H. J. Garrett, "X-Ray Studies of Tetragonal-Monoclinic Inversion in ZrO_2," Bull. Amer. Ceram. Soc., 42 (4) 201 (1963).

21. A. Dietzel and H. Tober, "Zirconium Dioxide and Binary Systems with Zirconia as Component," Ber. Deut. Keram. Ges., 30 (3) 47-61; (4) 71-82 (1953); Ceram. Abstr., 1954, January, p. 23a.

22. F. A. Mumpton and R. Roy, "Low-Temperature Equilibria Among ZrO_2, ThO_2, and UO_2," J. Am. Ceram. Soc., 43 (5) 234-40 (1960).

23. R. Ruh, H. J. Garrett, R. F. Domagala, and N. M. Tallan, "The System Zirconia-Hafnia," J. Am. Ceram. Soc., 51 (1) 23-27 (1968).

24. L. L. Fehranbacher and L. A. Jacobson, "Metallographic Observation of the Monoclinic-Tetragonal ZrO_2 Phase Transformation," Bull. Am. Ceram. Soc., 43 (4) 257 (1964); J. Am. Ceram. Soc., 48 (3) 157-61 (1965).

25. R. F. Geller and P. J. Yavorsky, "Effects of Some Oxide Additions on Thermal-Length Changes of Zirconia," J. Research Natl. Bur. Standards, 35 (1) 87-110 (1945); Ceram. Abstr., 24 (10) 191 (1945).

26. C. E. Curtis, L. M. Doney, and J. R. Johnson, "Some Properties of Hafnium Oxide, Hafnium Silicate, Calcium Hafnate, and Hafnium Carbide," J. Am. Ceram. Soc., 37 (10) 458-65 (1954).

27. P. Murray and E. B. Allison, "Study of Monoclinic ⇄ Tetragonal Phase Transformation in Zirconia," Trans. Brit. Ceram. Soc., 53 (6) 335-61 (1954).

28. B. C. Weber and M. A. Schwartz, "Zirconium Oxide-Its Crystal Polymorphism and Suitability as a Super-refractory," Ber. Deut. Keram. Ges., 34 (12) 391-96 (1957); Ceram. Abstr., 1958, June, p. 148e.

29. P. Duwez, F. Odell and F. H. Brown, Jr., "Stabilization of Zirconia with Calcia and Magnesia," J. Am. Ceram. Soc., 35 (5) 107-13 (1952).

30. R. C. Garvie, "The Cubic Field in the System CaO-ZrO_2," J. Am. Ceram. Soc., 51 (10) 553-56 (1968).

31. R. Roy, H. Miyabe, and A. M. Diness, "Subsolidus Decomposition of CaO-'Stabilized' ZrO_2," Bull. Am. Ceram. Soc., 43 (4) 255 (1964).

32. B. C. Weber, H. J. Garrett, F. A. Mauer, and M. A. Schwartz, "Observations on the Stabilization of Zirconia," J. Am. Ceram. Soc., 39 (6) 197-207 (1956).

33. R. C. Garvie and P. S. Nicholson, "Phase Analysis in Zirconia Systems," paper submitted to J. Am. Ceram. Soc., Sept., 1971.

34. W. J. Campbell and C. F. Grain, U.S. Bur. Mines, RI 5982 (1962).

35. S. M. Lang, "Axial Thermal Expansion of Tetragonal ZrO_2 Between 1150° and 1700°C," J. Am. Ceram. Soc., 47 (12) 641-44 (1964).

36. C. E. Curtis, "Development of Zirconia Resistant to Thermal Shock," J. Am. Ceram. Soc., 30 (6) 180-96 (1947).

37. C. F. Grain, "Phase Relations in the ZrO_2-MgO System," J. Am. Ceram. Soc., 50 (6) 288-90 (1967).

VIII. VITA

Damri Sukhotanang was born on September 6, 1949, in Petchburi, Thailand. He received his elementary and secondary education in that town.

He attended college at Chulalongkorn University, Bangkok, Thailand, receiving a Bachelor of Science degree with Second Class Honours in Ceramics Technology, Department of Chemical Technology, in April 1969.

He was employed as an instructor by the Department of Chemical Technology, Faculty of Science, Chulalongkorn University, Bangkok, Thailand, during the period June 1969 to June 1970.

He has been enrolled in the Graduate School of the University of Missouri-Rolla, continuing graduate study in the Department of Ceramic Engineering since August, 1970 and has held a scholarship from Thailand.

He is a member of the American Ceramic Society and Keramos.